Biophysical Chemistry 123 (2006) 58–76

Biophysical Chemistry

http://www.elsevier.com/locate/biophyschem

Mechanochemical couplings of kinesin motors

Ping Xie *, Shuo-Xing Dou, Peng-Ye Wang

Laboratory of Soft Matter Physics, Beijing National Laboratory for Condensed Matter Physics, Institute of Physics, Chinese Academy of Sciences, Beijing 100080, China

Received 12 January 2006; received in revised form 3 April 2006; accepted 8 April 2006
Available online 26 April 2006

Abstract

Kinesins are molecular motors capable of moving processively along microtubule in a stepwise manner by hydrolyzing ATP. Numerous experimental results on various aspects of their dynamical behaviours are available in literature. Although a number of models of tightly coordinated mechanism have been proposed to explain some experimental results, up to now no good explanation has been given to all these experimental results by using a single model. We have recently proposed such a model of partially coordinated hand-over-hand moving mechanism. In this paper, we use this model to study in detail various aspects of the dynamical properties of single kinesin molecules. We show that kinesin dimers walk hand-over-hand along microtubules in a partially coordinated rather than a tightly coordinated manner. The degree of coordination depends on the ratio of the two heads' ATPase rates that are in turn determined by both internal elastic force and external load. We have tested this model using various available experimental results on different samples and obtained a good agreement between the theory and the experiments.

Keywords: Kinesin; Dynamics; Mechanism; Model

1. Introduction

A conventional kinesin is a two-headed protein that converts chemical energy of ATP hydrolysis to mechanical force and plays important roles in transporting membrane-bound vesicles and organelles in various cells. For the purpose of transport, it moves unidirectionally along a microtubule (MT) for hundreds of ~8-nm steps without dissociating [1–5]. Since its discovery, kinesin has been studied extensively by using various experimental methods [6–12]. In particular, by using optical trapping nanometry, many aspects of its dynamics such as the mean movement velocity, randomness, mean run length, backward stepping and limping behaviours under various loads and ATP concentrations have been elaborately studied [2,3,13–25].

So far the microscopic mechanism of the processive movement of kinesin has not been well understood. There are now mainly two types of models in literature. One type is the thermal ratchet model in which a motor is simply viewed as a Brownian particle moving in two (or more) spatially periodic but asymmetric stochastically switched potentials [26–28]. Since the conventional kinesin has two heads, the thermal ratchet model is too simple to give detailed descriptions to the moving mechanism of the conventional kinesin such as the relations of the two heads during the movement. This model is more suitable for modeling the processive movement of single-headed motors such as the unconventional single-headed kinesin KIF1A [29,30]. Another prevailing type of models for conventional kinesin are the hand-over-hand models [1,7,8,10–12,21,31–39]. In these models, it is supposed that the kinesin dimer maintains continuous attachment to MT by alternately repeating single-headed and double-headed bindings. Recent experiments [21,39] strongly support this type of models by revealing that kinesin walks in an asymmetric hand-over-hand manner and a given head of the dimer is displaced in discrete steps with a mean size of ~16 nm. All these models require that the two heads move in a *tightly coordinated* manner. Based on this tight-coordination assumption, some of the dynamical behaviours has been systematically studied in theory by Fisher and his colleagues [40,41].

* Corresponding author.
E-mail address: pxie@aphy.iphy.ac.cn (P. Xie).

0301-4622/$ - see front matter © 2006 Elsevier B.V. All rights reserved.
doi:10.1016/j.bpc.2006.04.003

Recently, we propose a new hand-over-hand model for the conventional kinesin dimer [42,43], in which the ATPase activities of the two heads are *partially coordinated*, in contrast to *tightly coordinated* as required by the previous models. We have shown that the degree of coordination is dependent on the load and mutant vs. wild type: Under a low load, the wild-type motor steps forward processively with, in general, one ATP being hydrolyzed per step (1 : 1 coupling). This movement of the dimer with 1 : 1 mechanochemical coupling results solely from the fact that the ATPase rate of the trailing head is much higher than the leading head, which is caused by the different forces acting on the two heads (the trailing head being pulled forward and the leading head backward). Under a large forward load or for some mutant kinesins even under no load, the ATPase activities of the two heads do not behave in a well-coordinated way, with more than one ATP molecule being consumed for making a forward step.

To verify this model, in this work, we will apply it to study quantitatively diverse dynamical properties of single kinesin molecules such as the dependence of mean velocity on [ATP], [ADP], [Pi], temperature and load, the dependence of mean run length on [ATP] and load, the dependence of stall force on [ATP], the effect of sideways force, the backward stepping behaviours. The calculated results are in good agreement with experiments.

2. Movement mechanism

Our model for the processive movement of a two-headed kinesin motor along MT has been described in detail in our previous paper [43]. Before making a detailed comparison between the results obtained from this model and those of available experiments, let us first briefly describe the model itself.

We begin with the dimeric kinesin in rigor state as shown in Fig. 1(a) or Fig. 1(a′), where the trailing head is in ATP state and the leading head is in nucleotide-free state. Kinesin in this state has a larger free energy than in the equilibrium (or free) state as shown in Fig. 1(d) or Fig. 1(e′), which corresponds to the state having the minimum free energy. Minimization of free energy requires that the kinesin tends to change from the rigor state to its equilibrium state via an internal elastic force and an internal elastic torque between the two heads. As discussed in detail in our previous work [43], the conformational change from the rigor state [e.g., Fig. 1(a′)] to the equilibrium state [e.g., Fig. 1(e′)] is associated with the docking of the neck linker of the leading head, which accompanies a large free energy change for the dimer, while for a monomer the free energy change associated with the docking of the neck linker of the head accompanies a small free energy change. This prediction is in qualitative agreement with experiments in which the free energy change is measured to be small for the monomer [44] and large for the dimer [45].

The rigor state as shown in Fig. 1(a) or Fig. 1(a′) can evolve in two different ways: Either the ATP in the trailing head can be hydrolyzed earlier than an ATP to be bound to the leading head, or an ATP binds to the leading head earlier than the ATP in the trailing head being hydrolyzed. We thus consider the two cases separately.

2.1. Effective mechanochemical cycle

ATP hydrolysis occurs at the trailing head [Fig. 1(b)]. After ATP hydrolysis, Pi release [Fig. 1(c)] results in the weakening of electrostatic binding force between the trailing head and the binding site (I) of MT, which is assumed to be resulted from the conformational changes both in the MT-binding site of the kinesin head and in the kinesin-binding site (I) of MT to which the kinesin head is bound [30]. From this and driven by the internal elastic force and torque, the trailing head is then detached from MT and moves to its equilibrium position, as shown in Fig. 1(d). In this equilibrium state, there exists only an electrostatic interaction force between the positively charged detached kinesin head and the neighboring negatively charged tubulin heterodimer (III). This interaction force drives the detached head coming close to heterodimer (III) (which gives a very short stepping time even at very low [ATP] [24,46]). Since the neck linker of the trailing head that is in nucleotide-free state cannot be docked to the head domain, the leading head cannot bind to the binding site (III), which inhibits ADP release [47], as shown in Fig. 1(e). After ATP binds to the trailing head, its neck linker is docked to the head domain, thus allowing the leading head binding to MT and then releasing ADP, as shown in Fig. 1 (f). From Fig. 1(a) to (f) a mechanochemical cycle is completed, with one ATP being consumed for an effective mechanical step.

2.2. Futile mechanochemical cycle

ATP binds to the leading head as shown in Fig. 1(b′). ATP hydrolysis [Fig. 1(c′)] and then Pi release occur earlier at the leading head than the trailing head [Fig. 1(d′)]. The leading head becomes detached and then the dimeric kinesin is changed from the state in Fig. 1(d′) to the equilibrium state in Fig. 1(e′). After the conformation in the kinesin-binding site (II) of MT tubulin where the leading head has just been detached relaxes to its normal form with a relaxation time, t_r, the leading head rebinds to the binding site (II), as shown in Fig. 1(f′). One ATP is hydrolyzed in this futile mechanical cycle.

In the following, we will make all calculations based on this model.

3. Dynamics

Since the moving time in one step is much shorter than the ATPase time [24,42], the mean movement velocity of kinesin, V, is essentially dependent only on ATPase rates of the two heads. The ATPase cycling of a given head is described by the following scheme

$$\text{Empty} \xrightarrow{k_1} \text{ATP} \xrightarrow{k_2} \text{ADP.Pi} \xrightarrow{k_3} \text{ADP} \xrightarrow{k_4} \text{Empty}, \quad (1)$$

where Empty represents nucleotide-free state, $k = k_b^{(\text{ATP})}$ [ATP] is the ATP-binding rate, k_2 the ATP-hydrolysis rate, k_3 the Pi-release rate and k_4 the ADP-release rate. For simplicity, we have

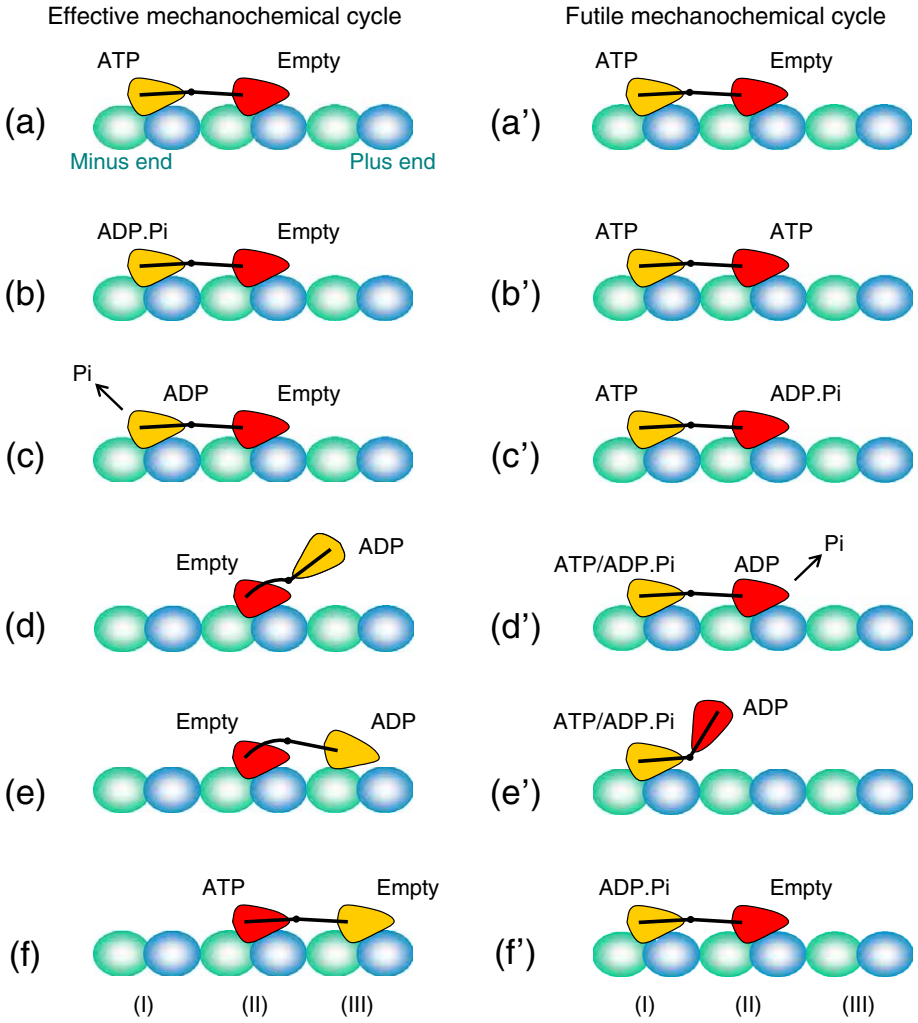

Fig. 1. Schematic illustrations of kinesin movement. *Effective mechanochemical cycle*: (a) The cycle begins with both heads binding to MT with the yellow head (trailing head) in ATP state and the red head (leading head) in nucleotide-free state. (b) ATP is hydrolyzed at the trailing head. (c) Pi is released from the trailing head. (d) The trailing head is detached and driven, by the internal elastic force, towards the position that corresponds to the equilibrium state of the dimer. (e) The new leading head (yellow) is driven close to the new binding site (III) via its electrostatic interaction with the binding site (III). Because the neck linker of the nucleotide-free new trailing head (red) cannot be docked, the ADP-bound leading head is inhibited from binding to the binding site (III). (f) After ATP binding to the trailing head, its neck linker is docked, allowing the leading head binding to MT and releasing ADP. *Futile mechanochemical cycle*: (a′) Kinesin is in the same state as that in (a). (b′) ATP binds to the leading red head. (c′) ATP is hydrolyzed at the leading head. (d′) Pi is released from the leading head. (e′) The leading head is detached and driven towards the position that corresponds to the equilibrium state of the dimer via the internal elastic force. (f′) The leading head rebinds to binding site (III) and releases ADP. (For interpretation of the references to colour in this figure legend, the reader is referred to the web version of this article.)

neglected the backward transitions in Scheme (1) because each backward-transition rate is much smaller than the corresponding forward-transition rate in the case of no ADP and Pi [10]. The effects of ADP and Pi will be studied in Section 9.

The effect of a force, F, acting on the neck linker of a kinesin head on its chemical reaction rates should follow the general kinetics of an enzymatic reaction, which is in the general Boltzmann form [42,43,48], i.e.,

$$k_i = \frac{k_i^{(0)}(1+A_i)}{1+A_i\exp(F\delta_i^{(+)}/k_BT)}, \tag{2a}$$

$$k_i = \frac{k_i^{(0)}(1+A_i)}{1+A_i\exp(F\delta_i^{(-)}/k_BT)}, \qquad (i=b,\,2,\,3,\,4) \tag{2b}$$

where Eq. (2a) is for the case that the neck linker is pointed forward or a net forward force is acted on the neck linker [e.g., the trailing head in Fig. 1(a) or (a′)], while Eq. (2b) is for the case that the neck linker is pointed backward or a net backward force is acted on the neck linker [e.g., the leading head in Fig. 1 (a) or (a′)]. The force F is defined as positive when it is minus-end pointed and negative when it is plus-end pointed, which is consistent with the definition of load usually adopted in the literature. The parameters $\delta_i^{(+)}$ and $\delta_i^{(-)}$ are the characteristic distances for the forward and backward forces, respectively. Note that when $A_i=0$ or $\delta_i=0$, $k_i=k_i^{(0)}$ is independent of load and when $A_i \gg 1$ the two equations are reduced to $k_i=k_i^{(0)}\exp(-F\delta_i^{(+)}/k_BT)$ and $k_i=k_i^{(0)}\exp(-F\delta_i^{(-)}/k_BT)$. In rigor state as shown in Fig. 1(a) and (a′), the force F can be written as

$$F = F_{\text{load}}/2 - F_0, \tag{3a}$$

when the head is trailing and

$$F = F_{\text{load}}/2 + F_0, \tag{3b}$$

when the head is leading, where F_{load} is the load acting on the coiled coil that connects the two heads through their neck linkers and F_0 is the magnitude of the internal elastic force. The signs of F_{load} is defined the same as that of F. We will study the dynamics of kinesin for the cases of backward (or positive) and forward (or negative) loads separately. It should be mentioned that a factor of 2 has been missed in the above expressions for F in our previous work [43]. But by halving the values of F_0 and doubling the values of δ given there, all the calculated results will remain unchanged.

3.1. Backward load

As will be seen below, under a backward (or positive) load, the ATP-binding rate $k_b^{(\text{ATP})}$ and ATP-turnover rate $k_c = k_2k_3/(k_2+k_3)$ of the trailing head are usually much higher than the corresponding rates of the leading head. Thus, according to the model, it is a very good approximation that, during the processive movement of kinesin under a backward load, we can neglect ATP binding (thus also ATP hydrolysis and Pi release) of the leading head. Due to the high ADP-release rate [34], ADP is considered to release rapidly from the leading head upon binding to MT. Therefore, under a backward load, the dwell period of kinesin in one step during its processive movement corresponds to the following scheme for the *trailing* head [Fig. 1(d), through (e), (f), (a) and (b), to (c)]

$$\text{Empty} \xrightarrow{k_1} \text{ATP} \xrightarrow{k_2} \text{ADP.Pi} \xrightarrow{k_3} \text{ADP}. \tag{4}$$

In the following, we denote the probabilities for finding the trailing head in Empty, ATP, ADP.Pi and ADP states by ϕ, T, DP, and D respectively. From Scheme (4), the probabilities are described by the following differential equations

$$\frac{\mathrm{d}\phi}{\mathrm{d}t} = -k_1\phi, \tag{5a}$$

$$\frac{\mathrm{d}T}{\mathrm{d}t} = k_1\phi - k_2T, \tag{5b}$$

$$\frac{\mathrm{d}(\text{DP})}{\mathrm{d}t} = k_2T - k_3(\text{DP}), \tag{5c}$$

$$\frac{\mathrm{d}D}{\mathrm{d}t} = k_3(\text{DP}). \tag{5d}$$

By solving Eq. (5a, b, c, d), with the initial conditions at $t=0$: $\phi(0)=1$, $T(0)=0$, DP(0)=0 and $D(0)=0$, we obtain the probability density for the dwell time, $f(t)=\mathrm{d}D/\mathrm{d}t$, as follows

$$f(t) = k_1k_2k_3\left(\frac{e^{-k_1t}}{(k_1-k_2)(k_1-k_3)} + \frac{e^{-k_2t}}{(k_2-k_1)(k_2-k_3)} + \frac{e^{-k_3t}}{(k_3-k_1)(k_3-k_2)}\right). \tag{6}$$

From Eq. (6), the mean dwell time is $T_d = 1/k_1 + 1/k_2 + 1/k_3$. Thus the mean movement velocity of the kinesin is approximately $V = d/T_d$, i.e.,

$$V = \frac{k_c[\text{ATP}]}{k_c/k_b^{(\text{ATP})} + [\text{ATP}]}d, \tag{7}$$

where $k_c = k_2k_3/(k_2+k_3)$ is the ATP-turnover rate and $d = 8\,\text{nm}$ is the step size.

3.2. Forward load

The discussion in Section 3.1 is for the case of a positive load. In this section, we will discuss the case of a negative (forward) load. As we will see in Section 4, for some kinesins, an increase in the magnitude of the forward load results in an increase in the ATPase rate of the leading head. On the other hand, the ATPase rate of the trailing head is already saturated even under zero load. Thus, the ATPase rate of the leading head may become comparable to that of the trailing head with the increase of the forward load. So we must also consider the contribution of the ATPase activity of the leading head to the kinesin movement.

Consider that the forward load is in such a range that the ATP binding and then ATP hydrolysis of the leading head can be completed before Pi release from the trailing head. Since the leading head will become a new trailing head in the successive mechanical cycle, the contribution to the kinesin movement from ATP binding and then ATP hydrolysis of the leading head is equivalent to increasing the chemical reaction rate of ATP binding and then ATP hydrolysis of the new trailing head. Thus the mean moving velocity of kinesin can be written as $V = Kd$, with K being approximately obtained by following equations (see Appendix A)

$$\frac{1}{K} = \frac{1}{k_{\text{eff}}^{\text{T}}} + \frac{1}{k_3^{\text{T}}}, \tag{8a}$$

$$k_{\text{eff}}^{\text{T}} = \frac{k^{\text{T}} + k^{\text{L}}}{1 - k^{\text{L}}/k_3^{\text{T}}}, \tag{8b}$$

$$\frac{1}{k^{\text{T}}} = \frac{1}{k_1^{\text{T}}} + \frac{1}{k_2^{\text{T}}}, \tag{8c}$$

$$\frac{1}{k^{\text{L}}} = \frac{1}{k_1^{\text{L}}} + \frac{1}{k_2^{\text{L}}} + \frac{1}{k_4^{\text{L}}}, \tag{8d}$$

where k_i^{T} and k_i^{L} ($i=1$, 2, or 4) denote rates k_i of the trailing and leading heads, respectively, and they are determined by Eqs. (2a, b) and (3a, b).

Note that Eq. (8a, b, c, d) is only an approximation. For precise calculations of V, we can use the following procedure. Focus on a given kinesin head (note that, during the processive movement of the kinesin, this given head acts as the trailing head and the leading head alternatively). As mentioned above, the ATPase activity of this head can be

described by Scheme (4) if the short time taken by the rapid ADP release is neglected. Thus the probability density of the time taken by an ATPase cycle of this head is described by Eq. (6). This equation also describes the probability density of the time taken by an ATPase cycle of the other head. From our model we know that when the ATPase cycle is finished at a trailing head, i.e., the Pi is released from the trailing head, a forward step will be made and the next ATPase cycle of this head will start as the head is leading; whereas when the ATPase cycle is finished at a leading head, the kinesin will make no step and, then, the next ATPase cycle of this head will start, after a relaxation time t_r, as the head is still leading. Therefore, the mean movement velocity of kinesin can be written either as

$$V = d/T_1, \tag{9a}$$

or as

$$V = (d/T_2)P^{\mathrm{T}}, \tag{9b}$$

where T_1 represents the mean time between two successive moments when Pi release occurs at the trailing head, T_2 represents the mean time between two successive moments when Pi release occurs at either of the two heads and P^{T} is the probability for occurrence of Pi release at the trailing head.

4. Mean velocity

The dependences of the mean velocity V on ATP concentration and on load have been studied in Xie et al. [43], where only the results for the case of backward loads have been fitted to the experimental results. Here we extend the study to fit the experimental results for the case of forward loads. In addition, we will use the same parameters that are used to fit the mean velocity to calculate the randomness, mean run length and stall force and to compare them with the experimental results by Visscher et al. [16,17]. For clarity we will first present the results for the mean velocity.

We first study the mean velocity V under a backward (or positive) load F_{load}. Using Eqs. (2a), (3a) and (7), the experimentally measured V vs. [ATP] under different loads by Visscher et al. [16] can be fitted very well, as seen in Fig. 2(a). The values of parameters for rates of ATP binding, ATP hydrolysis and Pi release used for the fitting are given in Table 1. The details of how these parameters and those in other tables are chosen will be discussed later in the Discussion Section. Using the same parameter values and Eqs. (2a), (3a) and (7), we calculate V vs. F_{load} at two ATP concentrations, the results of which are shown in Fig. 2(b). The theoretical results are in good agreement with the experimental ones.

Now, using Eqs. (2a, b) and (3a, b) we calculate the chemical reaction rates vs. load (both positive and negative) of the two heads with $\delta_i^{(+)} = \delta^{(-)}$ and the other parameter values given in Table 1. The calculated ATP-binding rate $k_{\mathrm{b}}^{(\mathrm{ATP})}$ and ATP-turnover rate $k_{\mathrm{c}} = k_2k_3/(k_2+k_3)$ of the two heads as a function of F_{load} are shown in Fig. 3. (For the case of $\delta_i^{(-)}=0$, $k_{\mathrm{b}}^{(\mathrm{ATP})}$ and k_{c} of the leading head are load independent, with the

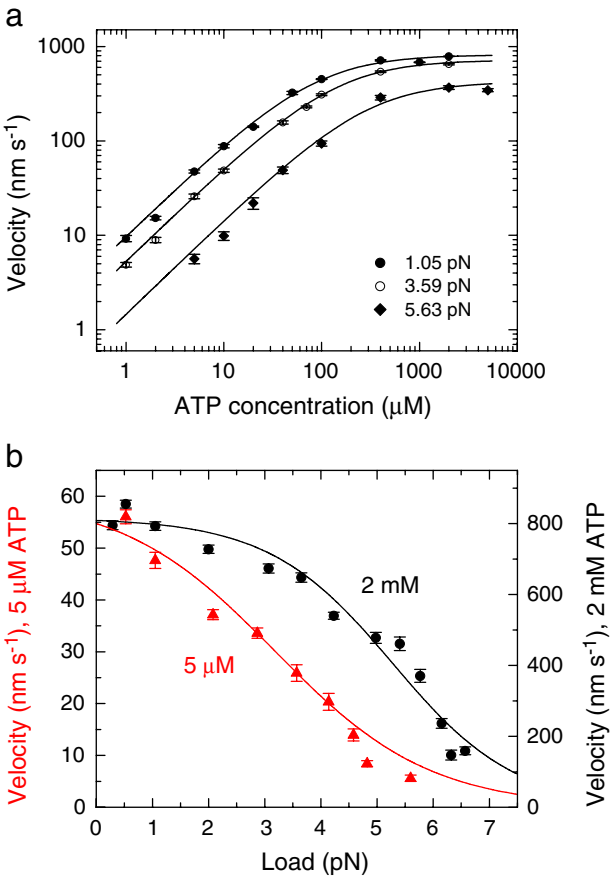

Fig. 2. (a) Velocity vs. [ATP] at various loads. (b) Velocity vs. load at different [ATP]. The data points are taken from Visscher et al. [16].

values equal to those of the trailing head under load $F_{\mathrm{load}} = 2F_0 = 6\,\mathrm{pN}$, i.e., $F = F_{\mathrm{load}}/2 - F_0 = 0$.) It is seen from Fig. 3 that, under a backward (positive) load, the chemical reaction rates of the trailing head are much higher than the corresponding rates of the leading head. Note also that, under no load, the ATP-binding rate, $k_{\mathrm{b}}^{(\mathrm{ATP})}$, of the leading head is much smaller than that of the trailing head for case of either $\delta_i^{(+)} = \delta_i^{(-)}$ or $\delta_i^{(-)} = 0$. This is consistent with the experimental results [38,49].

Here it is interesting to make a comparison of the chemical reaction rates calculated by using the parameter values given in Table 1 with that measured in bulk assays [34]. From the values in Table 1, we calculate the chemical reaction rates of a kinesin head with $F_{\mathrm{load}} = 0$. Using Eqs. (2a) and (3a) the obtained ATP-binding rate is $k_{\mathrm{b}}^{(\mathrm{ATP})} \approx 1.5\,\mu\mathrm{M}^{-1}\,\mathrm{s}^{-1}$, the ATP-hydrolysis rate is $k_2 = 260\,\mathrm{s}^{-1}$ and the Pi-release rate is $k_3 \approx 175\,\mathrm{s}^{-1}$ for the trailing head. These values are comparable to the measured ATP-binding rate of $\sim 2\,\mu\mathrm{M}^{-1}\,\mathrm{s}^{-1}$, ATP-hydrolysis rate of $\sim 100\,\mathrm{s}^{-1}$ and Pi-release rate of $\sim 50\,\mathrm{s}^{-1}$ for *Drosophila* kinesin [34].

The mean velocity V under a forward (or negative) load F_{load} can also be compared. Using Eqs. (2), (3), (8) and values of parameters given in Table 2 we calculate V vs. F_{load} for different ATP concentrations. The results are shown in Fig. 4. It is noted that the double-sigmoid shapes of the theoretical curves show

Table 1
Parameter values used for fitting the experimental results of Visscher et al. [16,17] for kinesin purified from squid optic lobe

$k_b^{(0)}$ ($\mu M^{-1}s^{-1}$)	A_b	$\delta_b^{(+)}$ (nm)	$k_2^{(0)}$ (s^{-1})	A_2	$k_3^{(0)}$ (s^{-1})	A_3	$\delta_3^{(+)}$ (nm)	F_0 (pN)
0.176	8.2	6	260	0	44.9	2.94	7.8	3

Table 2
Parameter values used for fitting the experimental results of Coppin et al. [13] for native squid kinesin

$k_b^{(0)}$ ($\mu M^{-1}s^{-1}$)	$A_b=A_3$	$\delta_b^{(+)}=\delta_b^{(-)}=\delta_3^{(+)}=\delta_3^{(-)}$ (nm)	$k_2^{(0)}$ (s^{-1})	$A_2=A_4$	$k_3^{(0)}$ (s^{-1})	$k_4^{(0)}$ (s^{-1})	F_0 (pN)
0.68	0.6	16	58	0	18	100	2.1

very good resemblance to the experimental ones for native squid kinesin [13]. Note also that under no load, i.e., $F_{load}=0$, from Table 2 the obtained $k_b^{(ATP)}\approx 1.1\,\mu M^{-1}s^{-1}$, $k_2=58\,s^{-1}$, $k_3\approx 30.2\,s^{-1}$ for the trailing head and $k_4=100\,s^{-1}$ for the leading head are close to the measured ATP-binding rate of $\sim 2\,\mu M^{-1}s^{-1}$, ATP-hydrolysis rate of $\sim 100\,s^{-1}$, Pi-release rate of $\sim 50\,s^{-1}$ and ADP-release rate of $\sim 300\,s^{-1}$ for *Drosophila* kinesin [34]. However, with the tightly coordinated mechanism there has been no good explanation given to these puzzling double-sigmoid load-velocity curves although many efforts have been made. Note that, when the forward (negative) load is further increased in Fig. 4, the probability becomes high that Pi is released from the leading head, i.e., Pi release occurs before the leading head becomes the trailing head. Thus the probability of futile mechanochemical cycle becomes high, resulting in a decrease of the moving velocity. This explains qualitatively why the moving velocity starts to drop off when the forward load is further increased in the experiment [13]. All the above comparisons with experiments give a strong support to our proposed partially coordinated hand-over-hand mechanism between the two heads.

Different from the experimental results by Coppin et al. [13], the results for native *Loligo pealei* kinesin by Block et al. [20] show that the moving velocity does not increase as the forward load is increased (in the range of <8 pN). In our previous work [43] we have explained that this discrepancy may be due to different values of $k_b^{(0)}$, $k_c^{(0)}$, A_c and A_b with $\delta_i^{(-)}=\delta_i^{(+)}$. Alternatively, we can explain that the discrepancy may be due to different values of $\delta_i^{(+)}$ and $\delta_i^{(-)}$. For example, if taking $\delta_i^{(-)}=0$, $F_0=2.2$ pN, $k_b^{(0)}=0.156\,\mu M^{-1}s^{-1}$, $k_c^{(0)}=33.8\,s^{-1}$ and

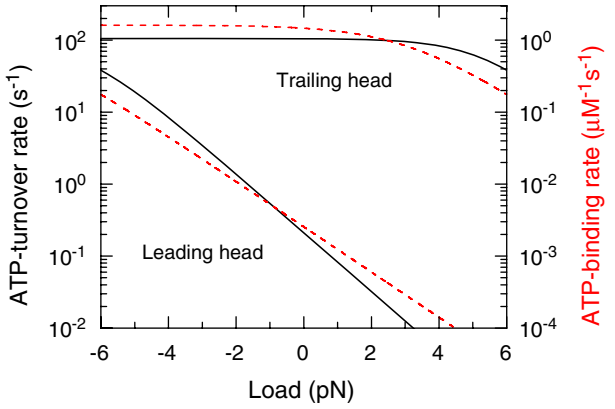

Fig. 3. ATP-turnover rate k_c (black solid lines) and ATP-binding rate k_b (dashed red lines) of the two heads as a function of F_{load}. (For interpretation of the references to colour in this figure legend, the reader is referred to the web version of this article.)

the other values of parameters (A_b, $\delta_b^{(+)}$, $A_c=A_3/[1+(1+A_3)k_3^{(0)}/k_2^{(0)}]=1.75$, $\delta_c^{(+)}=\delta_3^{(+)}$) from Table 1, we show the calculated results of velocity vs. load for different ATP concentrations in Fig. 5. The results are in agreement with the experimental ones. Note also that the values of F_0, $k_b^{(0)}$ and $k_c^{(0)}$ used here are close to but not exactly the same as the values obtained from Table 1 ($F_0=3$ pN, $k_b^{(0)}=0.176\,\mu M^{-1}s^{-1}$ and $k_c^{(0)}=k_2^{(0)}k_3^{(0)}/(k_2^{(0)}+k_3^{(0)})=38.3\,s^{-1}$). The slight difference in the values of parameters is reasonable by considering different experimental conditions. The different values of $\delta_i^{(+)}$ and $\delta_i^{(-)}$ can be due to the asymmetrical structure of the kinesin motor domain. As in the case that leftward and rightward forces give rise to different characteristic distances of $\delta_i^{(left)}$ and $\delta_i^{(right)}$ (see Block et al. [20] and Section 12), the forward and backward forces, i.e., the forward-pointed and backward-pointed neck linkers, may also give rise to different values of $\delta_i^{(+)}$ and $\delta_i^{(-)}$.

Note that the observed slight decrease of the mean velocity vs. forward load at saturating [ATP] [20] can be explained as follows. When a forward force is applied to the coiled-coil, besides a large forward component there always exists a small vertical component of the force acted on the trailing head [21]. As shown in Block et al. [20], the ATP-turnover rate k_c decreases with the increase of the sideways force while the sideways force has no or negligible effect on the ATP binding rate. If it is assumed that the vertical force has a similar effect on the ATP-turnover rate and negligible effect on the ATP binding rate, we have the following results: The small vertical component of the force would slightly reduce the mean velocity at saturating [ATP], because the velocity is saturated for the forward component of force (black line in Fig. 5), while the small vertical component of the force would have little effect on the velocity at low [ATP]. Thus the velocity at low [ATP] will not be reduced even at large forward load, which is in agreement with the experimental results [20]. Note that the phenomenon in the MT buckling experiment [50] that the kinesin motors speed up when the force became nonparallel to the direction of motor movement was well explained by also assuming the vertical force reducing the ATP-turnover rate for a given forward longitudinal load by Kim and Fisher [51].

5. Randomness

As defined in Schnitzer and Block [14] and Visscher et al. [16], the randomness, r, can be obtained by the equation

$$r=\left(\int_0^\infty t^2 f(t)\mathrm{d}t-\left(\int_0^\infty tf(t)\mathrm{d}t\right)^2\right)\Big/\left(\int_0^\infty tf(t)\mathrm{d}t\right)^2. \quad (10)$$

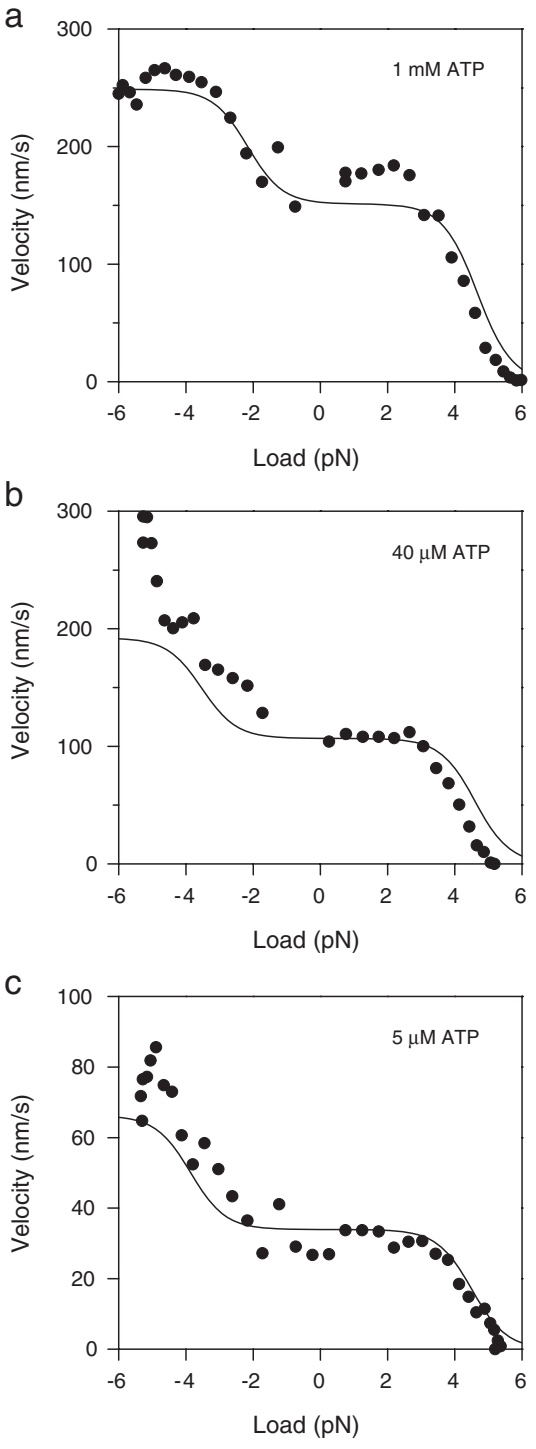

Fig. 4. Load–velocity curves at [ATP]=1 mM (a), 40 μM (b), and 5 μM (c). The data points are taken from Coppin et al. [13].

Substituting the dwell time distribution $f(t)$, Eq. (6), into Eq. (10), we obtain $r=(1/k_1^2+1/k_2^2+1/k_3^2)/(1/k_1+1/k_2+1/k_3)^2$, which can be rewritten as

$$r=\left(\frac{1}{\left(k_b^{(ATP)}[ATP]\right)^2}+\frac{1}{k_2^2}+\frac{1}{k_3^2}\right)\Big/\left(\frac{1}{k_b^{(ATP)}[ATP]}+\frac{1}{k_2}+\frac{1}{k_3}\right)^2. \quad (11)$$

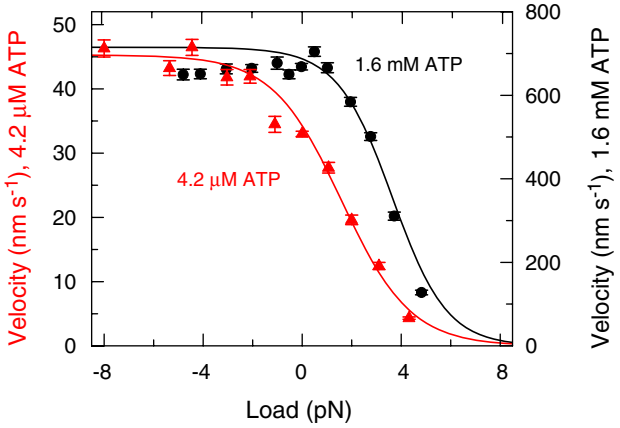

Fig. 5. Load–velocity curves at [ATP]=4.2 μM (a) and 1.6 mM (b). The data points are taken from Block et al. [20]. Note that present definition of load direction is opposite to that in Block et al. [20].

Using Eqs. (2a), (3a), (11) and the values of parameters given in Table 1, we calculate the randomness r vs. [ATP] and vs. F_{load}. The results are shown in Fig. 6. It is seen that the theoretical curves have similar shapes to the experimental ones by Visscher et al. [16]. Similarly, using the fitted parameter values for the experimental results by Block at al. [20] (in Fig. 5), the calculated results for randomness–load curves for two ATP concentrations are shown in Fig. 7, which also show good resemblance to the experimental ones by Block et al. [20]. According to the definition of r, its maximum values should be equal to one. The fact that the maximum value of the experimentally measured r is slightly larger than one may be due to other factors such as backward steps, enzyme inactivations and futile mechanochemical couplings [14,16].

6. Mean run length

As in experiment [17], we only consider the mean run length, L, in the case of backward load in this section. According to our model, during one step in the processive movement of kinesin, one has approximately three periods during which the kinesin has distinct probabilities to dissociate from MT: (1) The kinesin is in rigor state [e.g., Fig. 1(a)]. During this period, because both heads bind strongly to MT the kinesin has a very low probability, P_1, to dissociate from MT and thus we can approximately take $P_1\approx 0$. (2) The trailing head in nucleotide-free state binds strongly to MT and the leading head in ADP-state unable to bind MT [e.g., Fig. 1(e)]. During this period, the probability, P_2, of the kinesin dissociation from MT is proportional to the duration of this state and thus can be expressed as $P_2=p_2^{(0)}/k_b^{(ATP)}[ATP]$, where $p_2^{(0)}$ is the dissociation rate when only one head bound to MT in nucleotide-free state. (3) The period when Pi is released from the trailing head while the leading head is detached from MT due to a large backward load and the thermal noise. In this case the kinesin has a large probability of $P_3\approx 1$ to dissociate from MT.

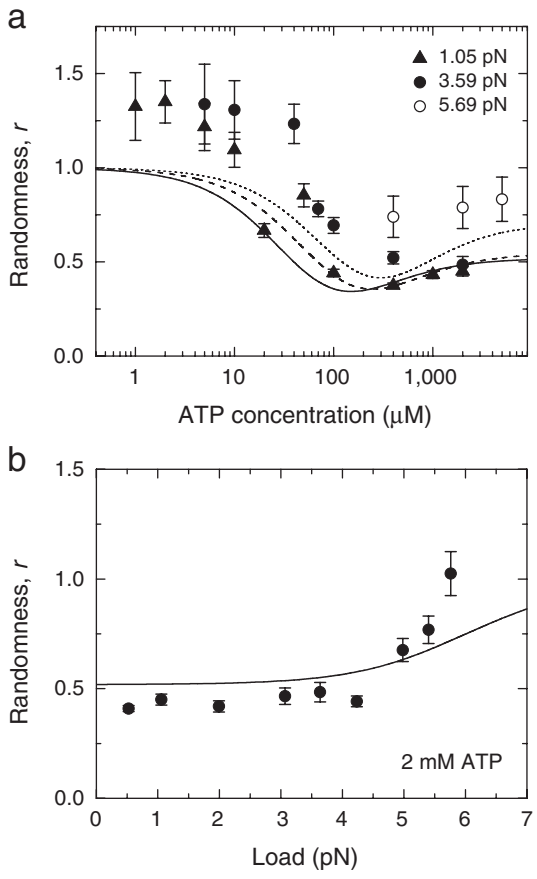

Fig. 6. (a) Randomness vs. [ATP] at loads of 1.05 pN (solid line), 3.59 pN (dashed line) and 5.69 pN (dotted line). (b) Randomness vs. load at [ATP]=2 mM. The data points are taken from Visscher et al. [16].

The mean run length, L, is inversely proportional to the sum of the above three dissociation probabilities, i.e. $L = \mathrm{d}/\sum_{i=1}^{3} P_i$, where d=8 nm is the step size. Thus we have

$$L = d\frac{[\mathrm{ATP}]}{p_2^{(0)}/k_\mathrm{b}^{(\mathrm{ATP})} + (P_1 + P_3)[\mathrm{ATP}]}. \tag{12}$$

As stated above, $P_1 \approx 0$ and $p_2^{(0)}$ is constant. According to Kramers [52], P_3 can be calculated by

$$P_3 = p_3^{(0)} \exp\left(\frac{(F_\mathrm{load}/2 + F_0)\delta_\mathrm{d}}{k_\mathrm{B}T}\right), \tag{13}$$

where $p_3^{(0)}$ is constant.

Using Eqs. (2a), (12) and (13) and values of F_0, $k_\mathrm{b}^{(0)}$, A_b and $\delta_\mathrm{b}^{(+)}$ given in Table 1, together with $p_2^{(0)} = 0.025\,\mathrm{s}^{-1}$, $p_3^{(0)} = 1\times10^{-4}$ and $\delta_\mathrm{d} = 3$ nm, we calculate the mean run length L vs. [ATP] and vs. F_load. The results are shown in Fig. 8. It is seen that they are in agreement with the experimental ones [17].

7. Stall force

In this section, we give an explanation to the experimentally obtained [ATP] dependence of the stall force, F_S, in Visscher et al. [16]. As did in experiment, we define that a load that can stall the kinesin for $t > t_\mathrm{S} = 2$ s corresponds to the stall force.

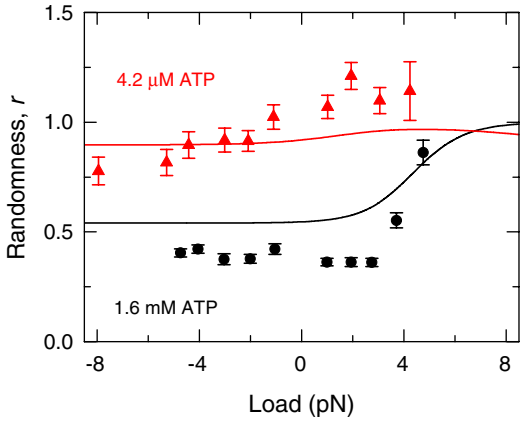

Fig. 7. Randomness vs. load at different [ATP]. The data points are taken from Block et al. [20]. Note that present definition of load direction is opposite to that in Block et al. [20].

According to the model, there are three cases that the kinesin can be stalled for $t > t_\mathrm{S}$: (1) When the time, T_dwell, of ATP binding, ATP hydrolysis and Pi release at the trailing head is longer than t_S, the kinesin will become stalled for $t > t_\mathrm{S} = 2$ s. (2) When the time, T_move, required for the trailing head to move a step after Pi release becomes longer than the

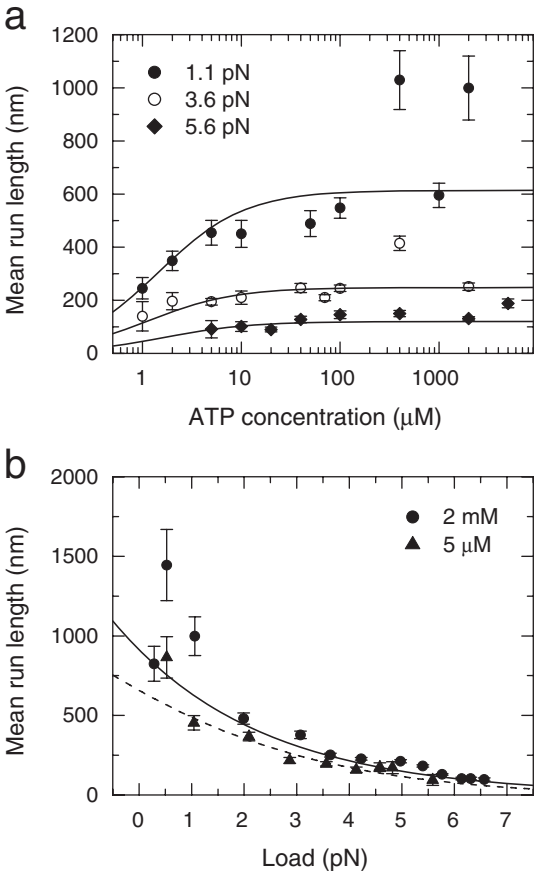

Fig. 8. (a) Mean run length vs. [ATP] at various loads. (b) Mean run length vs. load at [ATP]=2 mM (solid line) and 5 μM (dashed line). The data points are taken from Schnitzer et al. [17].

relaxation time t_r, as defined in Section 2, the kinesin cannot move forward because the trailing head will rebind to the binding site from which it has just been detached. (3) When the ratio of forward to backward steps is equal to 1, the kinesin on average cannot move. Therefore, the stall force corresponds to the minimum one among the load (F_{dwell}) that makes $T_{dwell} \approx t_S$, the load (F_{move}) that makes $T_{move} \approx t_r$ and the load (F_{ratio}) that makes the ratio of forward to backward steps becomes equal to 1.

T_{dwell} is obtained by the following equation

$$T_{dwell} = \frac{1}{k_b^{(ATP)}[ATP]} + \frac{1}{k_c}, \tag{14}$$

where $k_b^{(ATP)}$ and $k_c = k_2 k_3/(k_2+k_3)$ are obtained from Eqs. (2a) and (3) with F_{load} replaced by F_{dwell}. T_{move} is essentially the mean first-passage time for the trailing head to diffuse a distance of $2d = 16$ nm. T_{move} can be obtained by the following equation [42]

$$T_{move} = \frac{1}{f_{diff}}\left[\frac{D}{f_{diff}}\left(\exp\left(\frac{f_{diff}}{D}2d\right)-1\right)-2d\right], \tag{15}$$

where $f_{diff} = (F_{move}/2 - F_0')/\Gamma$ and $D = k_B T/\Gamma$. F_0' is the average driving force on the detached trailing head during its movement over the distance of 2d. Here $\Gamma = 6\pi\eta r_k = 5.65\times10^{-11}\,kg\,s^{-1}$, where the viscosity η of the aqueous medium is approximately $0.01\,g\,cm^{-1}\,s^{-1}$ and the kinesin head is treated as a sphere with radius $r_k \approx 3$ nm.

Using Eqs. (2a), (3a) and (14) and parameter values given in Table 1, the obtained F_{dwell} vs. [ATP] is shown by curve A–B–C in Fig. 9, where we take $T_{dwell} = 2$ s.

Using Eq. (15), we obtain $F_{move}/2 - F_0' \approx 2.65$ pN. As the driving force has the maximum value of $F_0 = 3$ pN, as an example, we take $F_0' = 1.5$ pN. We then have $F_{move} \approx 8.3$ pN, which is shown by line C–D in Fig. 9, where we take $T_{move} = t_r = 1.5$ ms that is the same as we have taken for single-headed kinesin KIF1A [30].

The ratio of forward to backward steps will be studied in Section 10, where it is shown that, to make the ratio of forward over backward steps equal to 1, the backward load $F_{ratio} = 2F_0 = 6$ pN for the case of $\delta_3^{(-)} = 0$ and saturating [ATP]. The result of $F_{ratio} = 6$ pN is shown by line B–E in Fig. 9. Therefore, the stall force corresponds to curve A–B–C–D in Fig. 9 if $\delta_3^{(-)} \neq 0$ and corresponds to curve A–B–E if $\delta_3^{(-)} = 0$. The theoretical results are in agreement with the experimental ones [16].

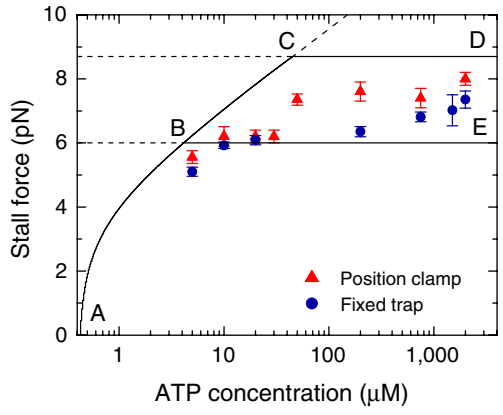

Fig. 9. Stall force vs. [ATP]. The data points are taken from Visscher et al. [16].

8. Unbinding force

Previous experimental results [53,54] on distributions of unbinding force show that, for single-headed kinesins, there is only one peak for distributions of unbinding force in the presence of either 1 mM ADP, or 1 mM AMP–PNP that is an ATP analog, or under nucleotide-free condition. For two-headed kinesins, there is also only one peak for distributions of unbinding force in the presence of 1 mM ADP or under nucleotide-free condition. However, in the presence of 1 mM AMP–PNP, there are two peaks for distributions of unbinding force.

Further experimental results [19] on distributions of unbinding force for two-headed kinesin molecules show that, at intermediate ADP concentrations where populations of strong and weak MT-binding kinesins coexist, backward loading increases the proportion of strong binding molecules, while forward loading increases the proportion of weak binding molecules [19]. Since the strong and weak binding populations correspond to nucleotide-free and ADP-bound molecules, respectively, the result means that backward loading increases the proportion of molecules in nucleotide-free population, while forward loading increases the proportion of molecules in ADP-bound population.

Now we give explanations to the above experimental results using our model and calculate the [ADP] dependence of the proportion of molecules in ADP-bound population. Since in nucleotide-free state the neck linkers cannot be docked, only one of the two heads, i.e., the trailing head, can bind to MT (as Fig. 1(e) but with the leading head in nucleotide-free state. Note that the orientations of the two nucleotide-free heads in this configuration are similar, which is consistent with the fluorescence polarization anisotropy measurements [55]). In ADP state, because of the weak binding force, the kinesin also most probably binds to MT with only one head. Thus, as for one-headed kinesin, there is only one peak for the distribution of unbinding force for two-headed kinesin in nucleotide-free state or in ADP state. However, in the presence of AMP–PNP, the MT-bound head, i.e., the trailing head, can be either in AMP–PNP state or in nucleotide-free state. If the trailing head is in AMP–PNP state, its neck linker can be docked and thus both heads can bind to MT simultaneously. If the trailing head is in nucleotide-free state, its neck linker cannot be docked and thus the other head cannot bind to MT. Therefore in the presence of AMP–PNP, there will be two peaks for distributions of unbinding force, with one peak corresponding to single-headed binding and the other one corresponding to two-headed binding [53,54].

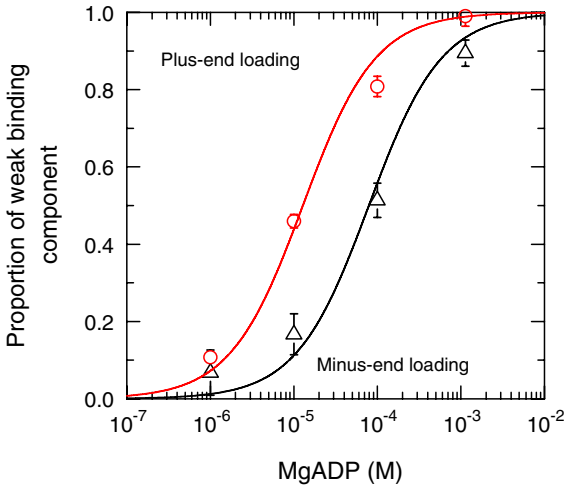

Fig. 10. Proportion of weak binding component vs. [MgADP] for plus-end loading of ~3.5 pN (black line) and minus-end loading of ~4 pN (red line). The data points are taken from Uemura and Ishiwata [19].

In the presence of ADP at intermediate concentration as in Uemura and Ishiwata [19], the proportion of kinesins in ADP-bound population, P, can be obtained by

$$P = \frac{P_D}{P_D + P_E}, \tag{16}$$

where P_D and P_E are probability for occurrence of ADP-bound state and that of nucleotide-free state, respectively. From scheme $\mathrm{ADP} \underset{k_{-4}}{\overset{k_4}{\rightleftharpoons}} \mathrm{Empty}$ we have the relation $P_E = (k_4/k_{-4})P_D$. Substituting this relation to Eq. (16) we obtain

$$P = \frac{[\mathrm{ADP}]}{k_4/k_b^{(\mathrm{ADP})} + [\mathrm{ADP}]}, \tag{17}$$

where $k_b^{(\mathrm{ADP})}$ is the ADP-binding rate relating to k_{-4} by $k_{-4} = k_b^{(\mathrm{ADP})}[\mathrm{ADP}]$. From the experimental results by Uemura and Ishiwata [19], the forward (plus-end) and backward (minus-end) unbinding forces in ADP-state are ~3.5 pN and ~4 pN, respectively. Using Eq. (17) we fit the experimental results [19], which are shown in Fig. 10, with the two fitted values of $K_0^{(\mathrm{ADP})} \equiv k_4/k_b^{(\mathrm{ADP})} = 12.9\,\mu\mathrm{M}$ and 79 μM under a forward load of 3.5 pN and a backward load of 4 pN, respectively. If we take $A_4 \gg 1, A_{-4} \gg 1$ and $\delta_4 = \delta_4^{(+)} = \delta_4^{(-)}$ in Eq. (2a, b), with the above two fitted values of $K_0^{(\mathrm{ADP})}$, we obtain $K_0^{(\mathrm{ADP})} = 30\,\mu\mathrm{M}$ for the kinesin head under no external force and $\delta_{-4} - \delta_4 = 2\,\mathrm{nm}$ at room temperature of 25 °C, where $\delta_{-4} = \delta_{-4}^{(+)} = \delta_{-4}^{(-)}$ is the characteristic distance for k_{-4}. Note that the value of $K_0^{(\mathrm{ADP})}$ obtained here is close to that obtained in the next section (Section 9).

9. Effect of ADP and phosphate

According to our model, in the presence of [ADP] and [Pi] and *under no load*, as in the experiment of Schief et al. [56], the dwell period of kinesin in one step of its processivity corresponds to the following scheme for the trailing head

where the trailing head is considered to be nucleotide free at the

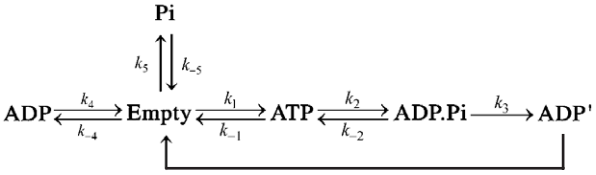

(18)

moment when it has just become trailing from the previous leading head because ADP-release rate of the leading head is high. ADP (or Pi) represents the ADP (or Pi) state due to ADP (or Pi) binding to the nucleotide-free trailing head that has been just become from the previous leading head. ADP′ represents the ADP state of the trailing head just after Pi is released. One important point to note is that, according to our model, the transition $\mathrm{ADP.Pi} \underset{k_{-3}}{\leftarrow} \mathrm{ADP}' + \mathrm{Pi}$ in the trailing head is impossible to occur, because upon Pi release (i.e., the transition $\mathrm{ADP.Pi} \overset{k_3}{\rightarrow} \mathrm{ADP}' + \mathrm{Pi}$) the trailing head is immediately driven to become the leading head by the internal force F_0 (see Section 2). In the absence of [ADP] and [Pi], Scheme (14) is reduced to Scheme (4) when we take $k_{-1} = 0$ and $k_{-2} = 0$.

From Scheme (18), the probabilities for finding the trailing head in ADP, Pi, ATP, ADP.Pi and ADP′ states are described, respectively, by the following differential equations

$$\frac{dD}{dt} = k_{-4}E - k_4 D, \tag{19a}$$

$$\frac{dP}{dt} = k_{-5}E - k_5 P, \tag{19b}$$

$$\frac{dT}{dt} = k_1 E - (k_{-1} + k_2)T + k_{-2}(\mathrm{DP}), \tag{19c}$$

$$\frac{d(\mathrm{DP})}{dt} = k_2 T - (k_3 + k_{-2})(\mathrm{DP}), \tag{19d}$$

$$\frac{dD'}{dt} = k_3(\mathrm{DP}), \tag{19e}$$

where $k_1 = k_b^{(\mathrm{ATP})}[\mathrm{ATP}]$, $k_{-4} = k_b^{(\mathrm{ADP})}[\mathrm{ADP}]$ and $k_{-5} = k_b^{(\mathrm{Pi})}[\mathrm{Pi}]$. From Eq. (19a–e) we obtain the mean chemical reaction rate for the process from ATP binding to Pi release

$$K = \frac{k_b^{(\mathrm{ATP})}[\mathrm{ATP}]}{A + Bk_b^{(\mathrm{ATP})}[\mathrm{ATP}]}, \tag{20a}$$

where

$$A = 1 + \frac{k_b^{(\mathrm{ADP})}[\mathrm{ADP}]}{k_4} + \frac{k_b^{(\mathrm{Pi})}[\mathrm{Pi}]}{k_5}, \tag{20b}$$

$$B = \frac{k_2 + k_3 + k_{-2}}{k_{-1}(k_{-2} + k_3) + k_2 k_3}. \tag{20c}$$

Table 3
Parameter values used for fitting the experimental results of Schief et al. [56] for native kinesin purified from bovine brain

$k_b^{(ATP)}$ ($\mu M^{-1} s^{-1}$)	k_2 (s^{-1})	k_3 (s^{-1})	$K_0^{(Pi)}=k_5/k_b^{(Pi)}$ (μM)	$K_0^{(ADP)}=k_4/k_b^{(ADP)}$ (μM)
4	300	200	10^4	30

As done in Sections 3 and 4, we can take $k_{-1}\approx 0$ and $k_{-2}\approx 0$ because they are much smaller than the corresponding forward transition rates k_1 and k_2. Thus Eq. (20c) is simplified to $B=(k_2+k_3)/k_2k_3=k_c^{-1}$. Then the mean movement velocity of kinesin can be written as

$$V = Kd = \frac{k_c[\mathrm{ATP}]}{Ak_c/k_b^{(\mathrm{ATP})} + [\mathrm{ATP}]}d. \tag{21}$$

Eq. (21) has the same form as Eq. (7), but with $Ak_c/k_b^{(ATP)}$ instead of $k_c/k_b^{(ATP)}$, which means that the presence of ADP and Pi approximately increases only the Michaelis–Menton constant K_m. Using Eqs. (20b) and (21) and parameter values given in Table 3, we calculate V as a function of [ATP], [ADP] and [Pi] under no load. The results are shown in Fig. 11. It is seen that the theoretical results are in good agreement with the experimental ones [56].

Note that, by using the tightly coordinated ADP-release-first hand-over-hand model [56], the experimental results can also be fitted well. However, the fitted value for Pi-release rate in the reaction of ADP.Pi→ADP′+Pi is $\sim 5600\,s^{-1}$ [56], which is significantly deviated from the measured value of $\sim 50\,s^{-1}$ [34]. On the contrary, by using our model of the partially coordinated hand-over-hand moving mechanism, the used values of $k_b^{(ATP)}=4\,\mu M^{-1}s^{-1}$, $k_2=300\,s^{-1}$ and $k_3=200\,s^{-1}$ for the trailing head given in Table 3 are close to the corresponding measured ones in bulk assays [34]. Note that these fitted parameter values given in Table 3 are also close to those from the single-molecule experimental results by Visscher et al. [16] ($k_b^{(ATP)}\approx 1.5\,\mu M^{-1}s^{-1}$, $k_2=260\,s^{-1}$, $k_3\approx 175\,s^{-1}$ as obtained from Table 1). Moreover, the equilibrium constant $K_0^{(ADP)}=30\,\mu M$ is also close to that determined in Section 8. This again supports our proposed partially coordinated hand-over-hand mechanism.

Similarly, by using Eqs. (20b) and (21) the experimental results of mean velocity (V) or mean dwell time (i.e., $1/V$) vs. [ATP] and/or [ADP] for rat kinesin by Yajima et al. [57] can also be fitted very well. At [ATP]=2 mM, the mean run length is simplified to $L=d/(P_1+P_3)$ (see Section 6), where both P_1 and P_3 is increased with the increase of [ADP] because ADP can bind to the two heads instead of ATP. Thus the mean run length will be decreased with the increase of [ADP], which is consistent with the experimental result [57].

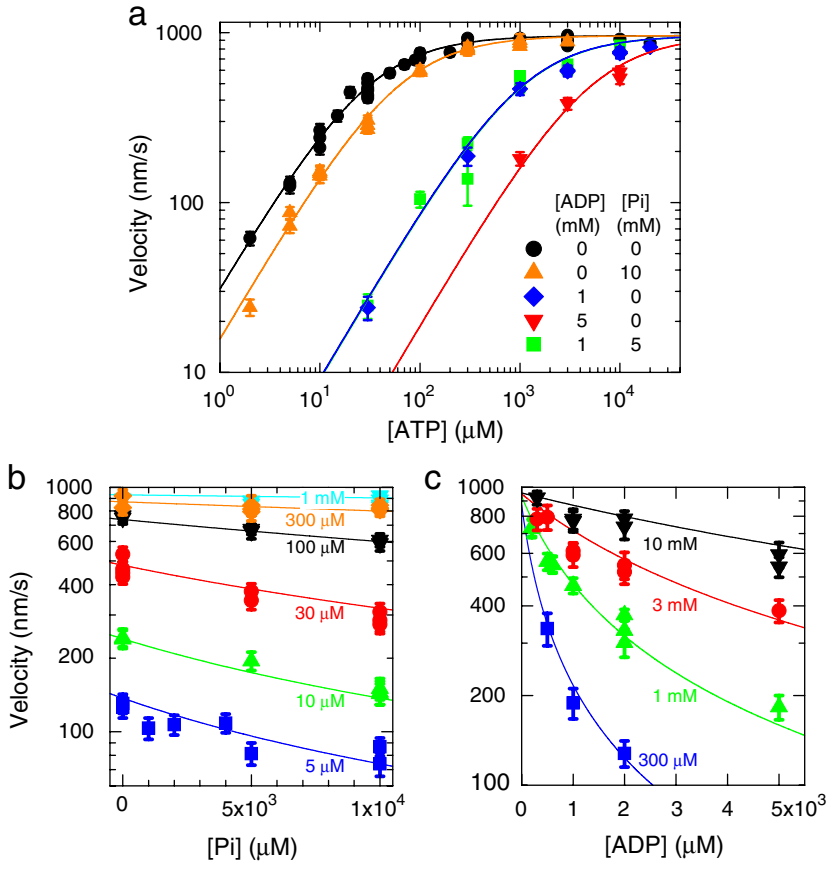

Fig. 11. (a) Velocity vs. [ATP] at various [ADP] and [Pi]. (b) Velocity vs. [Pi] at various [ATP]. (c) Velocity vs. [ADP] at various [ATP]. The data points are taken from Schief et al. [56].

A very recent experimental result showed that, in the presence of [ADP] and [Pi], ATP can be synthesized with a very slow rate [45]. According to our model, this synthesis of ATP can occur at both heads. If both ADP and Pi bind to the trailing head [see Fig. 1(e)], ATP can be synthesized at the head. If Pi binds to the detached leading head [see Fig. 1(e)], ATP can be synthesized at this head after the leading head is allowed to bind MT upon ADP binding to the trailing head. Furthermore, because the synthesis rate is negligibly slow even at [Pi]=10 mM (0.34 s^{-1}), it is a very good approximation that we can neglect it in Scheme (18) to analyze the effect of [ADP] and [Pi] on the mean velocity.

10. Backward stepping

Up to now we have taken the approximation that when Pi is released from the leading head the kinesin will make no stepping (i.e., a futile mechanochemical coupling). This is correct for the case of forward loads or very low backward loads. However, for the case that the backward load is not very low, the backward load, F_{load}, together with the thermal noise can overcome the internal force, F_0, to make the detached leading head diffuse backward and then binds to the previous binding site of MT. Thus a backward step is made, as schematically shown in Fig. 12. In detail, we described this case as follows.

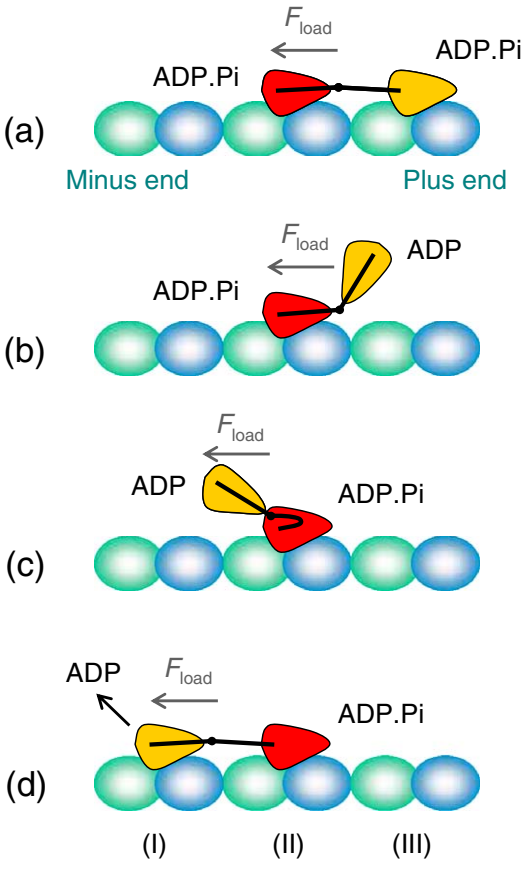

Fig. 12. Schematic illustration of a backward step under a backward load. (a) Both heads in ADP.Pi state. (b) Pi is released from the leading head earlier than from the trailing head and the leading is driven to its equilibrium position. (c) Under the influence of the backward load F_{load} and thermal noise, the detached head is moved to an intermediate position. (d) The detached head binds to the binding site (I) and then ADP will be released rapidly. From (a) to (b) a backward step has been made.

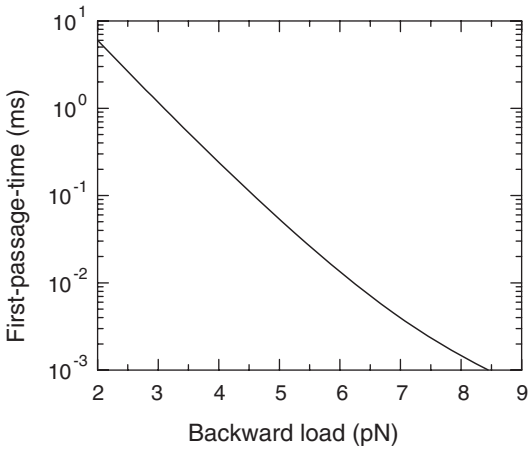

Fig. 13. The mean first-passage time vs. backward load of the detached head (yellow) from the position in Fig. 12(b) to that in Fig. 12(c).

Based on our model, after Pi is released from the leading head, the conformational changes in both the kinesin head and the binding site (III) induces the interaction force between the leading head and the binding site (III) becoming negligibly small. Thus the leading head is moved to the equilibrium position, as shown in Fig. 12(b). In this equilibrium conformation, there is only an external force, $F_{load}/2$, acting on the detached head. This backward load $F_{load}/2$ plus the thermal noise will overcome the internal force F_0 and thus the detached head is diffused to the binding site (I). Therefore, we have the following results: If the diffusing time of the detached head from Fig. 12(b) to (d) is longer than the relaxation time t_r of the binding site (III), the kinesin will rebind to binding site (III) and thus no stepping has been made. However, when the diffusing time is shorter than t_r, the detached head will bind to binding site (I) and thus a backward stepping is made.

Now we calculate the time, T_{diff}, taken for the detached leading head to diffuse from position shown in Fig. 12(b) to that shown in Fig. 12(d) over the distance of 13 nm (5 nm+8 nm), where 5 nm is the equilibrium distance between the two heads [58]. Using Eq. (15) with $f_{diff}=(F_0-F_{load}/2)/\Gamma$ we calculate T_{diff} vs. F_{load} at temperature of 25 °C for $\eta=0.01\,g\,cm^{-1}\,s^{-1}$, with the results shown in Fig. 13, where we take $F_0=4.5$ pN. It is seen that, for $F_{load}=2.2$ pN, $T_{diff}\approx 1.5$ ms, which is equal to $t_r=1.5$ ms [30]. Thus, for F_{load} that is smaller than 2.2 pN, the kinesin has a low probability to make backward stepping. However, for $F_{load}=2.5$ pN, $T_{diff}\approx 1$ ms, which is smaller than $t_r=1.5$ ms. Thus it can be considered that, for F_{load} that is larger than 2.5 pN, the kinesin can be considered to make a backward stepping when Pi is released from the leading head. In one word, when Pi is released from the trailing head a forward step will be made, whereas, for F_{load} that is larger than 2.5 pN, when Pi is

Table 4
Parameter values used for fitting the experimental results of Taniguchi et al. [25] for bovine brain kinesin

k_{20} ($s^{-1}K^{-1}$)	k_{30} ($s^{-1}K^{-1}$)	A_2	A_3	$\delta_3^{(+)}$ (nm)	$\delta_3^{(-)}$	$E_2^{(a)}$ (pNnm)	$E_3^{(a)}$ (pNnm)	F_0 (pN)
8.64×10^4	2.1×10^{11}	0	$\gg1$	5.4	0	49.2	128	4.5

released from the leading head a backward step will be made. Therefore, the forward stepping rate can be approximately calculated from ATP binding rate, ATP hydrolysis rate and Pi release rate of the trailing head, while the backward stepping rate can be approximately calculated from ATP binding rate, ATP hydrolysis rate and Pi release rate of the leading head because ADP release rate is much higher.

In the range of temperature $T<45\,°C$, the dependence of the chemical reaction rate of the kinesin head on temperature T should satisfy Arrhenius equation, i.e.,

$$k_i^{(0)} = k_{i0}T\exp\left(-\frac{E_i^{(a)}}{k_B T}\right), \tag{22}$$

where $E_i^{(a)}$ is the activation energy. Thus, we can use Eqs. (2), (3), (6) and (22) to calculate the dwell time distributions for forward and backward stepping, the forward and backward stepping rates and the ratio of forward to backward steps under various [ATP], backward loads F_{load} and temperatures T. In the case of saturating [ATP], the dwell time distributions and stepping rates are only dependent on the ATP-hydrolysis rate k_2 and Pi-release rate k_3. Their related parameter values are shown in Table 4. That means that, except that the dissociation rate is calculated from Eq. (13) with two parameters $p_3^{(0)}$ and δ_d, we will use only six parameters k_{20}, k_{30}, $\delta_3^{(+)}$, $E_2^{(a)}$, $E_3^{(a)}$ and F_0 to make all calculations in this section. From these parameters, the obtained ATP-hydrolysis rate is $k_2\approx164\,s^{-1}$ and Pi-release rate is $k_3\approx700\,s^{-1}$ ($F_{load}=0$) and $k_3\approx136\,s^{-1}$ ($F_{load}=2.5\,pN$). These values are close to those ($k_2=260\,s^{-1}$ and $k_3\approx175\,s^{-1}$) obtained from Table 1.

For example, the calculated dwell time distributions of the forward stepping under $F_{load}=4\,pN$ and temperatures of 7 °C and 35 °C are shown in Fig. 14(a), where the fast rise phase corresponds to ATP hydrolysis of the trailing head (with rate $k_2^{(Trail)}$) and it is independent of the loads, while the slow decay phase corresponds to Pi release of the trailing head (with rate $k_3^{(Trail)}$) and it is dependent on loads. The time constants, i.e., $1/k_2^{(Trail)}$ and $1/k_3^{(Trail)}$, vs. backward load F_{load} under temperatures of 7 °C and 35 °C are shown Fig. 14(b). It is important to note that, in our model, only when Pi is released from the leading head *earlier* than the trailing head can a backward step be made. Thus the mean dwell time for the backward steps should approximately equal to that for the forward steps and the load-dependent dwell time distributions for backward steps are nearly the same as that for forward steps. These are in agreement with the experimental results [18,24,25].

The forward and backward stepping rate constants that correspond to slow-decay phase in the dwell time distributions, i.e., $k_3^{(Trail)}$ and $k_3^{(Lead)}$, vs. backward load F_{load} under different

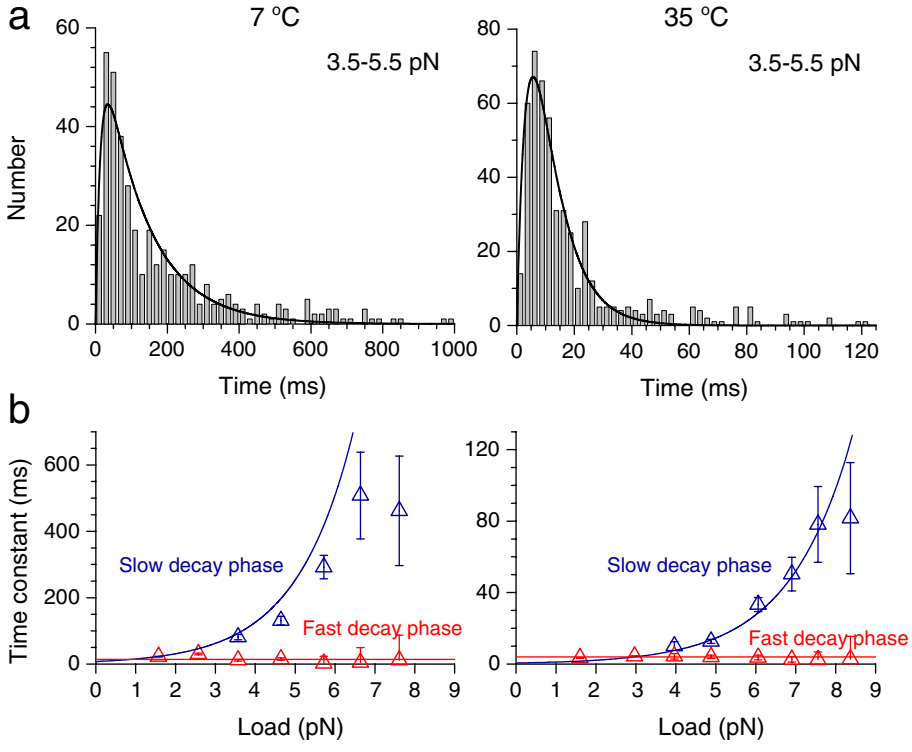

Fig. 14. Dwell time at different loads and temperatures. (a) Dwell time distributions under load of 4 pN at temperatures of 7 and 35 °C. (b) Dwell time constants vs. load at temperatures of 7 and 35 °C. The data points are taken from Taniguchi et al. [25].

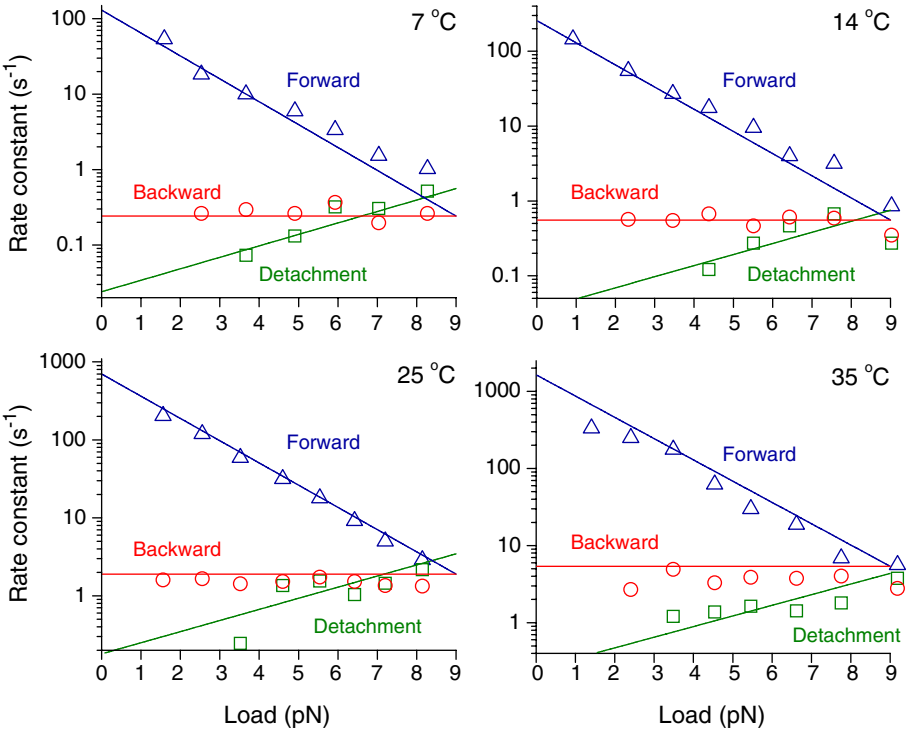

Fig. 15. The forward and backward stepping rate constants that correspond to the slow-decay phase in the dwell-time distributions vs. backward load F_{load} at different temperatures. The detachment rate is calculated by using $k_d \approx k_3^{(T)} P_3$, where P_3 is obtained from Eq. (13) with $\delta_d = 8.1$ nm and $p_3^{(0)} = 4.26\times10^{-3}$, 2.93×10^{-3}, 4.93×10^{-3}, 2.66×10^{-3} at temperatures of 7, 14, 25 and 35 °C, respectively. The data points are taken from Taniguchi et al. [25]. (For interpretation of the references to colour in this figure legend, the reader is referred to the web version of this article.)

temperatures are shown in Fig. 15. The results of $k_3^{(Trail)}$ and $k_3^{(Lead)}$ vs. temperature under no load are shown in Fig. 16. From $k_3^{(Trail)}$ and $k_3^{(Lead)}$ in Fig. 15 we can calculate the fraction of forward and backward steps by using $F_{forward} = k_3^{(Trail)}/(k_3^{(Trail)} + k_3^{(Lead)} + k_d)$ and $F_{backward} = k_3^{(Lead)}/(k_3^{(Trail)} + k_3^{(Lead)} + k_d)$, respectively, where k_d is the dissociation rate. The results are shown in Fig. 17. The ratio of forward to backward steps, $r_{f/b} = F_{forward}/F_{backward}$, is shown in the inset of Fig. 17 for temperature of 35 °C. It is seen that all the calculated results are in agreement with the experimental ones.

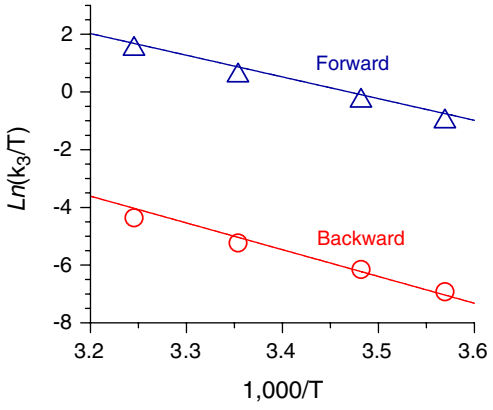

Fig. 16. The forward and backward stepping rate constants that correspond to slow-decay phase in the dwell-time distributions vs. temperature. The data points are taken from Taniguchi et al. [25].

Similarly, the experimental results for backward stepping behaviours by Carter and Cross [24] can also be fitted well with $F_0 = 3.6$ pN. Moreover, in Carter and Cross [24], it was experimentally shown that, under high backward loads larger than the stall force, the motor can walk backwards stepwise in a mode of ATP-dependent processivity. This can be easily explained as follows: For a backward load larger than $2F_0$ (i.e., the stall force), even if the process of Pi release is completed in the trailing head, the trailing head cannot or has a low probability to move forward to become the leading head due to the net backward force, i.e., $F = F_{load}/2 - F_0$, acting on the detached trailing head. However, when the process of Pi release is completed in the leading head, the kinesin can make a backward step. Therefore, under backward loads above stall force, the kinesin moves backwards stepwise and processively with the same ~8-nm step size as the forward stepping. Note that, during the processive backward stepping, ADP is released in the trailing head. Moreover, ATP binding is most probable to occur in the trailing head and Pi is most probable to release in the leading head. This mechanochemical cycle of the processive backward stepping is schematically shown in Fig. 18. Since ATP binding is involved, the dwell time of the processive backward stepping is thus ATP-dependent. Also, the backward stepping is coupled to ATP turnover, which needs further experimental verification.

Note that, in our model, the forward stepping is mainly caused by the internal force F_0 on the trailing head in rigor state (Fig. 1(c)), the internal electrostatic force between the faced surfaces of the two heads (Fig. 1(d)) and the weak electrostatic

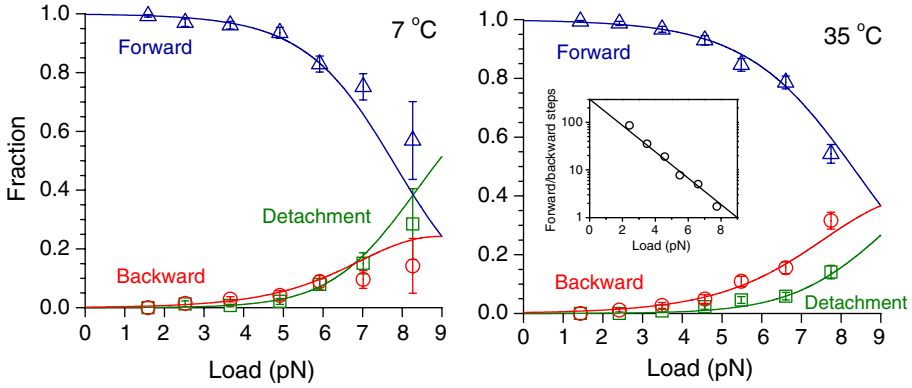

Fig. 17. Load dependence of the proportions of forward steps, backward steps and detachments. The inset is the ratio of forward to backward steps. The data points are taken from Taniguchi et al. [25].

force between the detached ADP-head and the next MT-tubulin heterodimer (Fig. 1(e)); while the backward stepping is mainly caused by the backward load together with the electrostatic interaction force between the detached ADP-head and the previous binding site (Fig. 12(d)). The direction of stepping is determined by whether Pi is released from the trailing head or from the leading head, rather than determined by an entropy asymmetry as suggested by Taniguchi et al. [25]. Note also that, with the tightly coordinated moving mechanism, it is difficult to explain the above experimental results of backward stepping behaviours. However, with our proposed partially coordinated mechanism, the backward stepping experimental results can be explained easily and quantitatively.

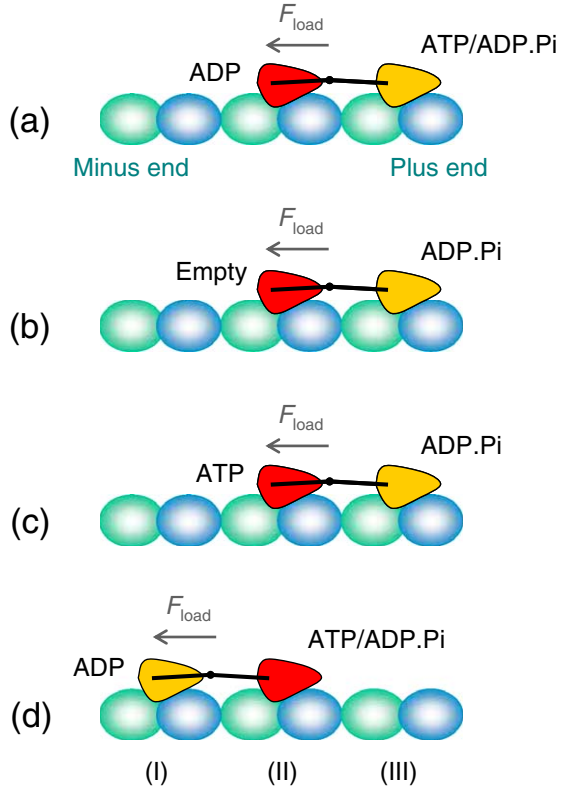

Fig. 18. Schematic illustration of processive backward stepping under a backward load F_{load} larger than the stall force. (a) The leading head (yellow) is in ATP or ADP.Pi state and the trailing head (red) in ADP state has been just become due to previous backward step. (b) Due to high ADP release rate, ADP is released rapidly from the trailing head. The leading head is still in ADP.Pi state due to low Pi release rate under a large backward load. (c) ATP binds to the nucleotide-free trailing head. (d) Upon Pi release from the previous leading head, it immediately becomes the new tailing head (yellow). The state of kinesin dimer in (d) becomes the same as that in (a) except a backward step has been made. Then the next backward step will be made. (For interpretation of the references to colour in this figure legend, the reader is referred to the web version of this article.)

11. Effect of temperature

In this section, we will study the dependence of mean movement velocity on both the temperature and the backward load in order to make comparisons between the theoretical results and the experimental results by Kawaguchi and Ishiwata [59].

Based on the discussion in the above section, the dependence of mean velocity on temperature and load at saturating [ATP] is described by $V=(k_c^{(Trail)}-k_c^{(Lead)})d$, where the ATP-turnover rates of the trailing head $k_c^{(Trail)}$ and the leading head $k_c^{(Lead)}$ are calculated from Eqs. (2), (3) and (22). Using the values of parameter given in Table 5, we calculate V as functions of temperature T and load F_{load}. The results are shown in Fig. 19(a) and (b). It is seen that the theoretical results are in good agreement with the experimental ones. In addition, based on our model, the internal elastic force F_0 is kept nearly constant with varying temperature for a given kinesin dimer. Thus, for the case of $\delta_c^{(-)}=0$, the stall force $F_S=2F_0=7.5$ pN (see Section 7) is nearly independent of the temperature, as shown in Fig. 19(c). The theoretical results are in agreement with the experimental one [59]. Note that if we take $E_c^{(a)}=E_2^{(a)}=E_3^{(a)}=82.8$ pN nm then we have $k_{c0}=k_{20}k_{30}/(k_{20}+k_{30})$. For $k_{c0}=5.94\times10^4\,s^{-1}K^{-1}$, we can decompose it

Table 5
Parameter values used for fitting the experimental results of Kawaguchi and Ishiwata [59] for bovine brain kinesin

k_{c0} ($s^{-1}K^{-1}$)	A_c	$\delta_c^{(+)}$ (nm)	$\delta_c^{(-)}$	$E_c^{(a)}$ (pN nm)	F_0 (pN)
5.94×10^4	3.6	3	0	82.8	3.75

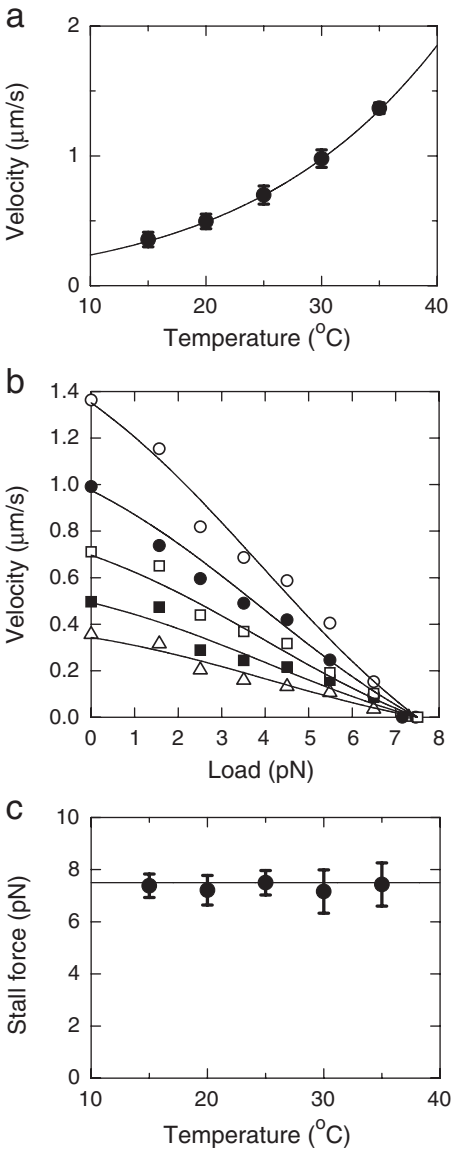

Fig. 19. (a) Velocity vs. temperature under no load. (b) Temperature dependence of load–velocity relation. From bottom to top, T=15, 20, 25, 30, 35 °C. (c) Stall force vs. temperature. The data points are taken from Kawaguchi and Ishiwata [59].

into $k_{20}\approx 5.94\times10^{4}\,s^{-1}K^{-1}$ and $k_{30}=2\times10^{11}\,s^{-1}K^{-1}$. These values of $E_2^{(a)}$, $E_3^{(a)}$, k_{20} and k_{30} are close to those given in Table 4.

12. Effect of sideways force

Similar to the effect of longitudinal force on the kinetics of a kinesin head, as discussed in Section 3, the effect of a sideways force on the chemical reaction rate of a kinesin head should also be in the general Boltzmann form

$$k_i^{(\mathrm{left})}=\frac{k_{i0}^{(\mathrm{sideways})}\left(1+A_i^{(\mathrm{left})}\right)}{1+A_i^{(\mathrm{left})}\exp\left(F^{(\mathrm{left})}\delta_i^{(\mathrm{left})}/k_BT\right)},\qquad(23a)$$

$$k_i^{(\mathrm{right})}=\frac{k_{i0}^{(\mathrm{sideways})}\left(1+A_i^{(\mathrm{right})}\right)}{1+A_i^{(\mathrm{right})}\exp\left(F^{(\mathrm{right})}\delta_i^{(\mathrm{right})}/k_BT\right)},$$

$$(i=b,\,2,\,3,\,4)\qquad(23b)$$

where $F^{(\mathrm{left})}(F^{(\mathrm{right})})$ is the leftward (rightward) force and $\delta_i^{(\mathrm{left})}(\delta_i^{(\mathrm{right})})$ is the characteristic distance for the leftward (rightward) force. $k_{i0}^{(\mathrm{sideways})}$ is the rate under no sideways force and, for the trailing head under no longitudinal load, it is

$$k_{i0}^{(\mathrm{sideways})}=\frac{k_i^{(0)}(1+A_i)}{1+A_i\exp(-F_0\delta_i^{(+)}/k_BT)}.\qquad(24)$$

As in the case of net forward and backward forces, since the kinesin head is not symmetrical, the dependences of the chemical reaction rate on the leftward and rightward forces may also be different.

Using parameter values for Fig. 5 and $A_b^{(\mathrm{left})}=A_b^{(\mathrm{right})}=0$, $A_c^{(\mathrm{left})}\gg1$, $A_c^{(\mathrm{right})}\gg1$, $\delta_c^{(\mathrm{left})}=0.23$ nm, $\delta_c^{(\mathrm{right})}=0.103$ nm, from Eqs. (23a, b) and (24) we calculate the mean velocity at different ATP concentrations and sideways forces. The results are shown in Fig. 20, which are in agreement with the experimental ones by Block et al. [20].

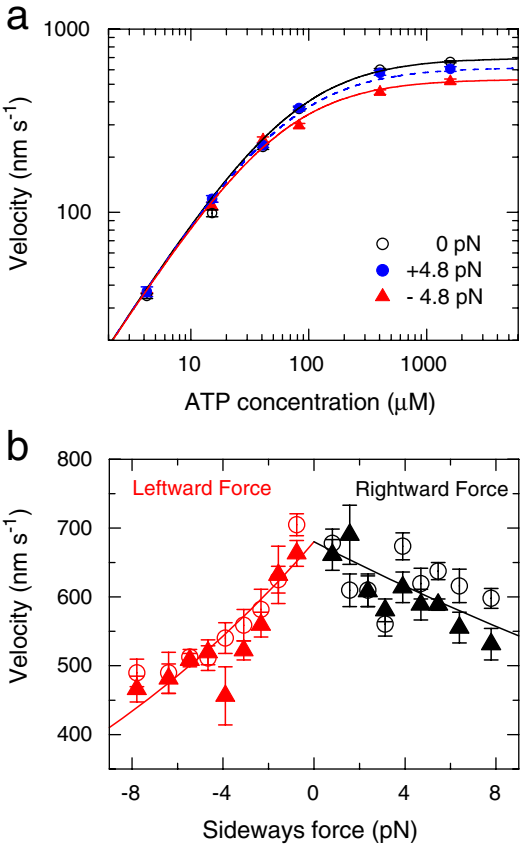

Fig. 20. (a) Velocity vs. [ATP] under sideways forces of 0 pN (solid black line), 4.8 pN (dashed blue line) and −4.8 pN (solid red line). (b) Velocity vs. sideways force at saturating [ATP]. The data points are taken from Block et al. [20]. (For interpretation of the references to colour in this figure legend, the reader is referred to the web version of this article.)

13. Discussion

Since some of the kinesin's dynamical behaviours have also be systematically studied by Fisher et al. [40,41], it is interesting to make comparisons between their model and our present model. First, in the former model an assumption of tight coordination between the two heads has been adopted. In our model, however, the two heads are partially coordinated in their ATPase activities: Under low loads, the two heads behave well coordinated, while under high loads the coordination of ATPase activities of the two heads is no longer well. Second, in the former model, the stepping direction is determined by the chemical reaction direction, which means that the kinesin dimer makes a forward mechanical step by consuming an ATP molecule while makes a backward step by synthesizing an ATP molecule. On the contrary, in our model, either the forward step or the backward step involves the consumption of an ATP molecule: When an ATP is hydrolyzed at the trailing head a forward step is made, while when an ATP is hydrolyzed at the leading head a backward step is made in the case of large backward loads. In the case of no or low loads, the much higher ATPase rate of the trailing head than the leading head assures that one ATP is generally consumed per step. However, under a large backward load, the ATPase rate of the leading head may become comparable to that of the trailing head, which leads to an increased ratio of backward over forward steps.

In Fisher and Kolomeisky [40] and Fisher and Kim [41], the direction of a stepping was determined by the chemical reaction direction. In other words, the synthesis of an ATP molecule induces a backward stepping while the hydrolysis of ATP produces a forward stepping. Another explanation [25] was that the direction of stepping was determined by an entropy asymmetry resulting from the compatibility between the kinesin and MT interaction. Different from these explanations, in our model the direction of stepping is explained to be determined by whether Pi is released from the trailing head or from the leading head. As we have seen in Section 10, the mathematical equations deduced from this model gave the results that show good quantitative agreement with the experimental ones. In particular, in our model the ATP binding is involved during the backward stepping, which is in agreement with the recent experimental result by Carter and Cross [24].

One may notice that the parameters we used in different tables (Tables 1–5) seem to be diverse. In fact, in the case of no ADP and Pi in the buffer, all the parameters in these tables can be obtained, through Eqs. (2a, b), (22) and $k_c=k_2k_3/(k_2+k_3)$, from the following set of 21 elementary parameters: k_{i0}, A_i, $\delta_i^{(\pm)}$, $E_i^{(0)}$ and F_0 , where $i=b$, 2, 3 and 4 that correspond to ATP binding, ATP hydrolysis, Pi release and ADP release, respectively. The different parameters used in Tables 1–5 just reflect the fact that the experiments are different in many aspects, that is, different experiments concern different behaviours of kinesin's dynamics so the minimum numbers of parameters required in each case are different. Furthermore, different experiments were done using different samples and the conditions in each experiment may be different. In the following, we explain how the 21 elementary parameters are reduced to the minimum numbers of parameters as given in Tables 1–5.

In the experiment of Taniguchi et al. [25] (Figs. 14–17), since the ATP concentration is saturated, due to the high ADP-release rate [34], we need only 11 parameters, i.e., k_{i0}, A_i, $\delta_i^{(\pm)}$, $E_i^{(a)}$ ($i=2$ and 3) and F_0. Furthermore, because of $A_2=0$, $\delta_2^{(\pm)}$ are not necessary and thus only 9 parameters as shown in Table 4 are needed.

In the experiment of Kawaguchi and Ishiwata [59] (Fig. 19), for the same reason as in the experiment of Taniguchi et al. [25], one should also need 11 parameters. However, through Eqs. (2a, b), (22) and $k_c=k_2k_3/(k_2+k_3)$, the 10 parameters (k_{i0}, A_i, $\delta_i^{(\pm)}$ and $E_i^{(a)}$, $i=2$ and 3) can be reduced to 5 parameters (k_{c0}, A_c, $\delta_c^{(\pm)}$ and $E_c^{(a)}$). Therefore, these 5 parameters plus F_0 as given in Table 5 are sufficient to fit the experimental results by Kawaguchi and Ishiwata [59]. As discussed in Section 11, the values of parameters in Table 4 are close to those in Table 5.

In the experiments of Coppin et al. [13] (Fig. 4), because the temperature was fixed, 8 parameters k_{i0} and $E_i^{(a)}$($i=b$, 2, 3 and 4) can be combined, through Eq. (22), to 4 parameters $k_i^{(0)}$. In addition, because of the high ADP-release rate, totally 13 parameters, i.e., $k_i^{(0)}$, A_i and $\delta_i^{(\pm)}$ ($i=b$, 2, 3) plus F_0, as shown in Table 2 are needed.

As in the experiments of Coppin et al. [13], to fit the experiment results by Visscher et al. [16,17] (Figs. 2, 6, 8 and 9), we should also need 13 parameters [$k_i^{(0)}$, A_i and $\delta_i^{(\pm)}$ ($i=b$, 2, 3), F_0]. However, because only backward loads are concerned in the experiments, the chemical reaction rates of the leading head are negligible compared to those of the trailing head (see Section 4) and thus 3 parameters from $\delta_i^{(-)}$ are redundant. In addition, as $A_2=0$, $\delta_2^{(+)}$ is also not required and therefore 9 parameters in total as shown in Table 1 are needed.

In the experiment of Schief et al. [56] (Fig. 11), if there is no ADP and Pi, we should need 13 parameters, $k_i^{(0)}$, A_i and $\delta_i^{(\pm)}$ ($i=b$, 2, 3) plus F_0, as in the experiments of Coppin et al. [13]. Because there is no external load, the 10 parameters $k_i^{(0)}$, A_i and $\delta_i^{(+)}$ ($i=b$, 2, 3) plus F_0 can be further reduced, through Eq. (2a, b), to 3 parameters k_i. In addition the 3 parameters from $\delta_i^{(-)}$ are redundant as just mentioned in the above. Due to the presence of ADP and Pi, two additional equilibrium constants for ADP and Pi are needed. Therefore, 5 parameters in total are necessary as shown in Table 3.

From the discussions above, we can see that the different sets of parameters used for fitting the experimental results from different sources are in fact originated from one same set of 21 elementary parameters. As shown in different sections where the values of parameters are used, from the values given in all the tables the calculated ATP-binding rate k_b, ATP-hydrolysis rate k_2, Pi-release rate k_3 and ADP-release rate k_4 of dimeric kinesins under no external load are close to those actually measured in bulk assays. In addition, the corresponding values of a given parameter in the different tables are also close. Thus it is possible to globally fit the general trend among the experiments shown in this paper using one set of parameter values. However, the fine structure of the results for each experiment may be different and cannot be well fitted because these experiments involve different samples and experimental conditions.

From the agreements between the diverse experimental results and the calculated results, we can have the following major conclusions about kinesin function: Kinesin dimers walk hand-over-hand along microtubules in a partially coordinated rather than a tightly coordinated manner. The degree of coordination depends on both internal elastic force and external load. Under no or low loads, the ATPase activities of the two heads are usually well coordinated due to their quite different reaction rates. Under high forward loads, the degree of coordination of ATPase activities of the two heads is reduced due to their comparable reaction rates. Under high backward loads, the degree of coordination is also reduced due to the high frequency of backward stepping. Both the forward and the backward stepping involve ATP binding and ATP turnover. When Pi is released from the trailing head a forward step is made. When Pi is released from the leading head under large backward loads, a backward step is made. In the cases of a forward load and of no or very low backward loads, when Pi is released from the leading head a futile mechanochemical coupling occurs.

14. Conclusion

Based on our proposed model of the partially coordinated hand-over-hand mechanism for the processive movement of conventional two-headed kinesins, we have studied in detail various dynamical behaviours of single kinesin molecules, such as the dependence of mean velocity on [ATP], [ADP], [Pi], temperature and load, the dependence of randomness and mean run length on [ATP] and load, the dependence of stall force on [ATP], the dependence of unbinding forces on [ADP], the effect of sideways force, the backward stepping behaviours, etc. Almost all the theoretical results show good agreement with the available experimental results. In particular, the puzzling experimental curves of velocity vs. load (both positive and negative) at different ATP concentrations for some kinesins and the dynamical behaviours of backward stepping are quite well explained.

The good agreements between the theoretical and experimental results on wild-type single kinesins, together with that on various mutant homodimers and heterodimers [22,60] as given in detail in our previous work [43], demonstrate the validity of our model of the partially coordinated hand-over-hand mechanism of kinesin. This view of partial coordination may also be applicable to other dimeric molecular motors such as myosin-V and myosin-VI.

Acknowledgment

This work was supported by the National Natural Science Foundation of China.

Appendix A. Derivation of Eq. (8a–d)

We begin with the moment when the trailing head just leaps forward and becomes the leading head. Assume the dwell time of kinesin between adjacent steps is t_{dwell} and neglect the leap time in each step, then t_{dwell} is the time for the leading head to release ADP, bind ATP and/or hydrolyze ATP. It is also the ATPase time for the trailing head, i.e.,

$$t_{\mathrm{dwell}} = \tau_{\mathrm{eff}}^{\mathrm{T}} + \tau_3^{\mathrm{T}}, \tag{A1}$$

where $\tau_3^{\mathrm{T}} = 1/k_3^{\mathrm{T}}$ and $\tau_{\mathrm{eff}}^{\mathrm{T}} = 1/k_{\mathrm{eff}}^{\mathrm{T}}$ is the time taken by the trailing head for ATP binding and/or ATP hydrolysis. As the trailing head has spent a time t_{dwell} as a leading head in previous cycle, it thus has a probability, $k^{\mathrm{L}} t_{\mathrm{dwell}}$, for ATP binding and/or hydrolysis, where k^{L} is defined in Eq. (8d). Thus $\tau_{\mathrm{eff}}^{\mathrm{T}}$ should satisfy

$$k^{\mathrm{L}} t_{\mathrm{dwell}} + k^{\mathrm{T}} \tau_{\mathrm{eff}}^{\mathrm{T}} = 1, \tag{A2}$$

where k^{T} is defined in Eq. (8c). From Eqs. (A1) and (A2), Eq. (9b) is obtained.

The effective ATPase time of the trailing head then is

$$T^{\mathrm{T}} = \tau_{\mathrm{eff}}^{\mathrm{T}} + \tau_3^{\mathrm{T}}, \tag{A3}$$

where $T^{\mathrm{T}} = 1/K$. After rewriting Eq. (A3) we obtain Eq. (8a).

References

[1] J. Howard, A.J. Hudspeth, R.D. Vale, Movement of microtubules by single kinesin molecules, Nature 342 (1989) 154–158.
[2] S.M. Block, L.S. Goldstein, B.J. Schnapp, Bead movement by single kinesin molecules studied with optical tweezers, Nature 348 (1990) 348–352.
[3] K. Svoboda, C.F. Schmidt, B.J. Schnapp, S.M. Block, Direct observation of kinesin stepping by optical trapping interferometry, Nature 365 (1993) 721–727.
[4] D.D. Hackney, Highly processive microtubule-stimulated ATP hydrolysis by dimeric kinesin head domains, Nature 377 (1995) 448–450.
[5] R.D. Vale, T. Funatsu, D.W. Pierce, L. Romberg, Y. Harada, T. Yanagida, Direct observation of single kinesin molecules moving along microtubules, Nature 380 (1996) 451–453.
[6] J. Howard, The movement of kinesin along microtubules, Annu. Rev. Physiol. 58 (1996) 703–729.
[7] S.M. Block, Leading the procession: new insights into kinesin motors, J. Cell Biol. 140 (1998) 1281–1284.
[8] R.D. Vale, R.A. Milligan, The way things move: looking under the hood of molecular motor proteins, Science 288 (2000) 88–95.
[9] R.A. Cross, Molecular motors: kinesin's interesting limp, Curr. Biol. 14 (2004) R158–R159.
[10] R.A. Cross, The kinetic mechanism of kinesin, Trends Biochem. Sci. 29 (2004) 301–309.
[11] C.L. Asbury, Kinesin: world's tiniest biped, Curr. Opin. Cell Biol. 17 (2005) 89–97.
[12] A. Yildiz, P.R. Selvin, Kinesin: walking, crawling or sliding along? Trends Cell Biol. 15 (2005) 112–120.
[13] C.M. Coppin, D.W. Pierce, L. Hsu, R.D. Vale, The load dependence of kinesin's mechanical cycle, Proc. Natl. Acad. Sci. U. S. A. 94 (1997) 8539–8544.
[14] M.J. Schnitzer, S.M. Block, Kinesin hydrolyzes one ATP per 8-nm step, Nature 388 (1997) 386–390.
[15] H. Kojima, E. Muto, H. Higuchi, T. Yanagida, Mechanics of single kinesin molecules measured by optical trapping nanometry, Biophys. J. 73 (1997) 2012–2022.
[16] K. Visscher, M.J. Schnitzer, S.M. Block, Single kinesin molecules studied with a molecular force clamp, Nature 400 (1999) 184–189.
[17] M.J. Schnitzer, K. Visscher, S.M. Block, Force production by single kinesin motors, Nat. Cell Biol. 2 (2000) 718–723.

[18] M. Nishiyama, H. Higuchi, T. Yanagida, Chemomechanical coupling of the ATPase cycle to the forward and backward movements of single kinesin molecules, Nat. Cell Biol. 4 (2002) 790–797.
[19] S. Uemura, S. Ishiwata, Loading direction regulates the affinity of ADP for kinesin, Nat. Struct. Biol. 4 (2003) 308–311.
[20] S.M. Block, C.L. Asbury, J.W. Shaevitz, M.J. Lang, Probing the kinesin reaction cycle with a 2D optical force clamp, Proc. Natl. Acad. Sci. U. S. A. 100 (2003) 2351–2356.
[21] C.L. Asbury, A.N. Fehr, S.M. Block, Kinesin moves by an asymmetric hand-over-hand mechanism, Science 302 (2003) 2130–2134.
[22] K. Kaseda, H. Higuchi, K. Horose, Alternate fast and slow stepping of a heterodimeric kinesin molecule, Nat. Cell Biol. 5 (2003) 1079–1082.
[23] H. Higuchi, C.E. Bronner, H.W. Park, S.A. Endow, Rapid double 8-nm steps by a kinesin mutant, EMBO J. 23 (2004) 2993–2999.
[24] N.J. Carter, R.A. Cross, Mechanics of the kinesin step, Nature 435 (2005) 308–312.
[25] Y. Taniguchi, M. Nishiyama, Y. Ishii, T. Yanagida, Entropy rectifies the Brownian steps of kinesin, Nat. Chem. Biol. 1 (2005) 342–347.
[26] R.D. Astumian, Thermodynamics and kinetics of a Brownian motor, Science 276 (1997) 917–922.
[27] F. Jülicher, A. Ajdari, J. Prost, Modeling molecular motors, Rev. Mod. Phys. 69 (1997) 1269–1281.
[28] R.D. Astumian, I. Derenyi, A chemically reversible Brownian motor: application to kinesin and Ncd, Biophys. J. 77 (1999) 993–1002.
[29] Y. Okada, H. Higuchi, N. Hirokawa, Processivity of the single-headed kinesin KIF1A through biased binding to tubulin, Nature 424 (2003) 574–577.
[30] P. Xie, S.-X. Dou, P.-Y. Wang, A non-Markov ratchet model of molecular motor: processive movement of single-headed kinesin KIF1A, Chin. Phys. 15 (2006) 536–541.
[31] C.S. Peskin, G. Oster, Coordinated hydrolysis explains the mechanical behavior of kinesin, Biophys. J. 68 (1995) 202s–210s.
[32] T. Duke, S. Leibler, Motor protein mechanics: a stochastic model with minimal mechanochemical coupling, Biophys. J. 71 (1996) 1235–1247.
[33] E. Mandelkow, K.A. Johnson, The structural and mechanochemical cycle of kinesin, Trends Biochem. Sci. 23 (1998) 429–433.
[34] S.P. Gilbert, M.L. Moyer, K.A. Johnson, Alternating site mechanism of the kinesin ATPase, Biochemistry 37 (1998) 792–799.
[35] W.O. Hancock, J. Howard, Kinesin's processivity results from mechanical and chemical coordination between the ATP hydrolysis cycles of the two motor domains, Proc. Natl. Acad. Sci. U. S. A. 96 (1999) 13147–13152.
[36] R.F. Fox, M.H. Choi, Rectified Brownian motion and kinesin motion along microtubules, Phys. Rev., E 63 (2001) 051901.
[37] S.A. Endow, D.S. Barker, Processive and nonprocessive models of kinesin movement, Annu. Rev. Physiol. 65 (2003) 161–175.
[38] L.M. Klumpp, A. Hoenger, S.P. Gilbert, Kinesin's second step, Proc. Natl. Acad. Sci. U. S. A. 101 (2004) 3444–3449.
[39] A. Yildiz, M. Tomishige, R.D. Vale, P.R. Selvin, Kinesin walks hand-over-hand, Science 303 (2004) 676–678.
[40] M.E. Fisher, A.B. Kolomeisky, Simple mechanochemistry describes the dynamics of kinesin molecules, Proc. Natl. Acad. Sci. U. S. A. 98 (2001) 7748–7753.
[41] M.E. Fisher, Y.C. Kim, Kinesin crouches to sprint but resists pushing, Proc. Natl. Acad. Sci. U. S. A. 102 (2005) 16209–16214.
[42] P. Xie, S.-X. Dou, P.-Y. Wang, Mechanism for unidirectional movement of kinesin, Chin. Phys. 14 (2005) 734–743.
[43] P. Xie, S.-X. Dou, P.-Y. Wang, Model for kinetics of wild-type and mutant kinesins, Biosystems 84 (2006) 24–38.
[44] S. Rice, Y. Cui, C. Sindelar, N. Naber, M. Matuska, R. Vale, R. Cooke, Thermodynamic properties of the kinesin neck region docking to the catalytic core, Biophys. J. 84 (2003) 1844–1854.
[45] D.D. Hackney, The tethered motor domain of a kinesin–microtubule complex catalyzes reversible synthesis of bound ATP, Proc. Natl. Acad. Sci. U. S. A. 102 (2005) 18338–18343.
[46] M. Nishiyama, E. Muto, Y. Inoue, T. Yanagida, H. Higuchi, Substeps within the 8-nm step of the ATPase cycle of single kinesin molecules, Nat. Cell Biol. 3 (2001) 425–428.
[47] D.D. Hackney, Evidence for alternating head catalysis by kinesin during microtubule-stimulated ATP hydrolysis, Proc. Natl. Acad. Sci. U. S. A. 91 (1994) 6865–6869.
[48] M.D. Wang, M.J. Schnitzer, H. Yin, R. Landick, J. Gelles, S.M. Block, Force and velocity measured for single molecules of RNA polymerase, Science 282 (1998) 902–907.
[49] S.S. Rosenfeld, P.M. Fordyce, G.M. Jefferson, P.H. King, S.M. Block, Stepping and stretching: how kinesin uses internal strain to walk processively, J. Biol. Chem. 278 (2003) 18550–18556.
[50] F. Gittes, E. Meyhöfer, S. Baek, J. Howard, Directional loading of the kinesin motor molecule as it buckles a microtubule, Biophys. J. 70 (1996) 418–429.
[51] Y.C. Kim, M.E. Fisher, Vectorial loading of processive motor proteins: implementing a landscape picture, J. Phys., Condens. Matter 17 (2005) S3821–S3838.
[52] H.A. Kramers, Brownian motion in a field of force and the diffusion model of chemical reactions, Physika 7 (1940) 284–304.
[53] K. Kawaguchi, S. Ishiwata, Nucleotide-dependent single to double-headed binding of kinesin, Science 291 (2001) 667–669.
[54] S. Uemura, K. Kawaguchi, J. Yajima, M. Edamatsu, Y.Y. Toyoshima, S. Ishiwata, Kinesin–microtubule binding is dependent on both nucleotide state and loading direction, Proc. Natl. Acad. Sci. U. S. A. 99 (2002) 5977–5981.
[55] A.B. Asenjo, N. Krohn, H. Sosa, Configuration of the two kinesin motor domains during ATP hydrolysis, Nat. Struct. Biol. 10 (2003) 836–842.
[56] W.R. Schief, R.H. Clark, A.H. Crevenna, J. Howard, Inhibition of kinesin motility by ADP and phosphate supports a hand-over-hand mechanism, Proc. Natl. Acad. Sci. U. S. A. 101 (2004) 1183–1188.
[57] J. Yajima, M.C. Alonso, R.A. Cross, Y.Y. Toyoshima, Direct long-term observation of kinesin processivity at low load, Curr. Biol. 12 (2002) 301–306.
[58] F. Kozielski, S. Sack, A. Marx, M. Thormahlen, E. Schonbrunn, V. Biou, A. Thompson, E.-M. Mandelkow, E. Mandelkow, The crystal structure of dimeric kinesin and implications for microtubule-dependent motility, Cell 91 (1997) 985–994.
[59] K. Kawaguchi, S. Ishiwata, Temperature dependence of force, velocity, and processivity of single kinesin molecules, Biochem. Biophys. Res. Commun. 272 (2000) 895–899.
[60] K. Kaseda, H. Higuchi, K. Horose, Coordination of kinesin's two heads studied with mutant heterodimers, Proc. Natl. Acad. Sci. U. S. A. 99 (2002) 16058–16063.